Extraction and Parametrization of Isobaric Trinucleon Elastic Cross Sections and Form Factors

Scott Barcus

February 5^{th} 2019

The College of William & Mary, Jefferson Lab

Table of contents

1. Introduction
2. Experimental Setup
3. Cross Section Extraction
4. Global Fits
5. Conclusions

Introduction

Brief Overview of JLab Work

- Graduate work at JLab since 2013.

Brief Overview of JLab Work

- Graduate work at JLab since 2013.
- SEOP of polarized ^{3}He targets at W&M.

Figure 1: GRINCH Detector.

Brief Overview of JLab Work

- Graduate work at JLab since 2013.
- SEOP of polarized ^{3}He targets at W&M.
- Gas Ring ImagiNg CHerenkov (GRINCH):
  - Built and tested the mirror system.
  - Characterized the PMTs and assembled the detector.
  - Developed preliminary DAQ.
  - Tested and implemented VETROC boards allowing for real-time high rate triggering.

Figure 1: GRINCH Detector.

Brief Overview of JLab Work

- Graduate work at JLab since 2013.
- SEOP of polarized ^{3}He targets at W&M.
- Gas Ring ImagiNg CHerenkov (GRINCH):
  - Built and tested the mirror system.
  - Characterized the PMTs and assembled the detector.
  - Developed preliminary DAQ.
  - Tested and implemented VETROC boards allowing for real-time high rate triggering.
- Hall A for the Tritium Experiments:
  - Maintained and prepared VDCs and EM calorimeters.
  - Counting house script maintenance and development.
  - Shift work and analysis shifts.

Figure 1: GRINCH Detector.

Brief Overview of JLab Work

- Graduate work at JLab since 2013.
- SEOP of polarized ^{3}He targets at W&M.
- Gas Ring ImagiNg CHerenkov (GRINCH):
  - Built and tested the mirror system.
  - Characterized the PMTs and assembled the detector.
  - Developed preliminary DAQ.
  - Tested and implemented VETROC boards allowing for real-time high rate triggering.
- Hall A for the Tritium Experiments:
  - Maintained and prepared VDCs and EM calorimeters.
  - Counting house script maintenance and development.
  - Shift work and analysis shifts.
- Worked on many JLab experiments:
  - SRC X>2, A_1^n, GMp, Ar(e,e'p), DVCS, and the Tritium Experiments.

Figure 1: GRINCH Detector.

Elastic Electron Scattering

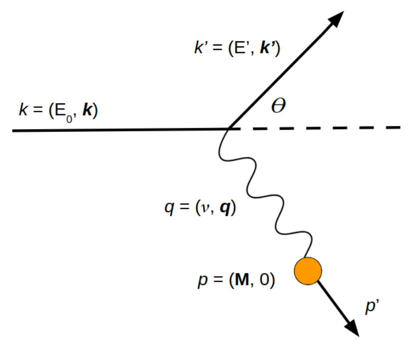

Figure 2: Elastic Electron Scattering. An incident electron interacts with a target by exchanging a virtual photon causing the electron to scatter.

$$\nu = E_0 - E' \tag{1}$$

$$E' = \frac{E_0}{1 + \frac{2E_0}{M} sin^2\left(\frac{\theta}{2}\right)} \tag{2}$$

$$Q^2 = -q^2 = 4E_0E'sin^2\left(\frac{\theta}{2}\right) \tag{3}$$

$$X_{Bj} = \frac{Q^2}{M(E_0 - E')} \tag{4}$$

Elastic Electron Scattering

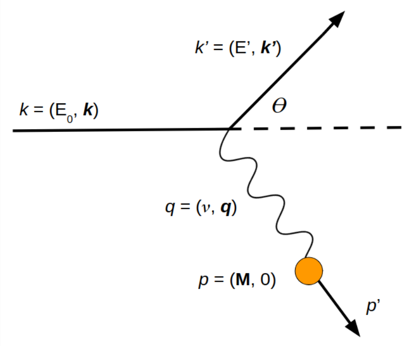

Figure 2: Elastic Electron Scattering. An incident electron interacts with a target by exchanging a virtual photon causing the electron to scatter.

$$\nu = E_0 - E' \tag{1}$$

$$E' = \frac{E_0}{1 + \frac{2E_0}{M} sin^2\left(\frac{\theta}{2}\right)} \tag{2}$$

$$Q^2 = -q^2 = 4E_0E' sin^2\left(\frac{\theta}{2}\right) \tag{3}$$

$$X_{Bj} = \frac{Q^2}{M(E_0 - E')} \tag{4}$$

- Elastic scattering is completely determined by knowing two of E_0, θ, or E'.

Rutherford Cross Section

- The differential cross section describes the likelihood of an electron interacting with a target.
  - Measures the 'size' of an interaction.
  - Must be viewed within a detector's solid angle acceptance.
- Rutherford Scattering: Charged particle scattering off a nucleus [1].

Rutherford Cross Section

- The differential cross section describes the likelihood of an electron interacting with a target.
  - Measures the 'size' of an interaction.
  - Must be viewed within a detector's solid angle acceptance.
- Rutherford Scattering: Charged particle scattering off a nucleus [1].

$$\left(\frac{d\sigma}{d\Omega}\right)_{Rutherford} = \frac{4Z^2\alpha^2\left(\hbar c\right)^2 E'^2}{|qc|^4} \tag{5}$$

Rutherford Cross Section

- The differential cross section describes the likelihood of an electron interacting with a target.
  - Measures the 'size' of an interaction.
  - Must be viewed within a detector's solid angle acceptance.
- Rutherford Scattering: Charged particle scattering off a nucleus [1].

$$\left(\frac{d\sigma}{d\Omega}\right)_{Rutherford} = \frac{4Z^2\alpha^2\left(\hbar c\right)^2 E'^2}{|qc|^4} \tag{5}$$

- Cross section falls off like $\frac{1}{q^4}$.
  - Likelihood of electrons interacting with a target decreases rapidly with energy.

Rutherford Cross Section

- The differential cross section describes the likelihood of an electron interacting with a target.
  - Measures the 'size' of an interaction.
  - Must be viewed within a detector's solid angle acceptance.
- Rutherford Scattering: Charged particle scattering off a nucleus [1].

$$\left(\frac{d\sigma}{d\Omega}\right)_{Rutherford} = \frac{4Z^2\alpha^2\left(\hbar c\right)^2 E'^2}{|qc|^4} \tag{5}$$

- Cross section falls off like $\frac{1}{q^4}$.
  - Likelihood of electrons interacting with a target decreases rapidly with energy.
- Rutherford equation does not account for relativity, spin, or target recoil.

Mott Cross Section

- Now add a term to account for relativity obtaining the Mott Equation [1]:

$$\left(\frac{d\sigma}{d\Omega}\right)_{\substack{\text{Mott}\\\text{No Recoil}}} = \left(\frac{d\sigma}{d\Omega}\right)_{Rutherford} \left(1 - \beta^2 sin^2\left(\frac{\theta}{2}\right)\right) \tag{6}$$

Mott Cross Section

- Now add a term to account for relativity obtaining the Mott Equation [1]:

$$\left(\frac{d\sigma}{d\Omega}\right)_{\substack{\text{Mott}\\ \text{No Recoil}}} = \left(\frac{d\sigma}{d\Omega}\right)_{Rutherford}\left(1-\beta^2 sin^2\left(\frac{\theta}{2}\right)\right) \tag{6}$$

- In the relativistic limit $\beta \to 1$ yielding [1]:

$$\left(\frac{d\sigma}{d\Omega}\right)_{\substack{\text{Mott}\\ \text{No Recoil}}} = \frac{4Z^2\alpha^2\left(\hbar c\right)^2 E'^2}{|qc|^4} cos^2\left(\frac{\theta}{2}\right) \tag{7}$$

Mott Cross Section

- Now add a term to account for relativity obtaining the Mott Equation [1]:

$$\left(\frac{d\sigma}{d\Omega}\right)_{\substack{\text{Mott}\\ \text{No Recoil}}} = \left(\frac{d\sigma}{d\Omega}\right)_{Rutherford}\left(1-\beta^2 sin^2\left(\frac{\theta}{2}\right)\right) \tag{6}$$

- In the relativistic limit $\beta \rightarrow 1$ yielding [1]:

$$\left(\frac{d\sigma}{d\Omega}\right)_{\substack{\text{Mott}\\ \text{No Recoil}}} = \frac{4Z^2\alpha^2\left(\hbar c\right)^2 E'^2}{|qc|^4} cos^2\left(\frac{\theta}{2}\right) \tag{7}$$

- Now we have accounted for relativity, but we have also accounted for spin with the $cos^2\left(\frac{\theta}{2}\right)$ term.
  - Suppresses scattering through 180° for a spinless target which is forbidden by conservation of helicity.

Mott Cross Section Cont.

- At our E_0 of 3.356 GeV an electron has 1.48 GeV of energy and a ^3He nucleus has a mass of 2.81 GeV.

Mott Cross Section Cont.

- At our E_0 of 3.356 GeV an electron has 1.48 GeV of energy and a ^{3}He nucleus has a mass of 2.81 GeV.
- Clearly neglecting recoil is no longer an option. Happily, the recoil term is easily found from Equation 2 describing elastic scattering

$$\frac{E'}{E_0} = \frac{1}{1 + \frac{2E_0}{M} sin^2\left(\frac{\theta}{2}\right)} \tag{8}$$

Mott Cross Section Cont.

- At our E_0 of 3.356 GeV an electron has 1.48 GeV of energy and a ^3He nucleus has a mass of 2.81 GeV.
- Clearly neglecting recoil is no longer an option. Happily, the recoil term is easily found from Equation 2 describing elastic scattering

$$\frac{E'}{E_0} = \frac{1}{1 + \frac{2E_0}{M} sin^2\left(\frac{\theta}{2}\right)} \quad (8)$$

- Now we can add the recoil term and rewrite the Mott cross section with a few substitutions from earlier as [1]:

$$\left(\frac{d\sigma}{d\Omega}\right)_{Mott} = \frac{4Z^2\alpha^2\left(\hbar c\right)^2 E'^3}{|qc|^4 E_0} cos^2\left(\frac{\theta}{2}\right) = Z^2 \frac{E'}{E_0} \frac{\alpha^2 cos^2\left(\frac{\theta}{2}\right)}{4E_0^2 sin^4\left(\frac{\theta}{2}\right)} \quad (9)$$

Nuclear Form Factors

- Now we have an equation that accounts for relativity, spin, and recoil off of a point mass.

Nuclear Form Factors

- Now we have an equation that accounts for relativity, spin, and recoil off of a point mass.
- Nuclei are not point masses! How do we describe the structure inside of a nucleus?

$$\left(\frac{d\sigma}{d\Omega}\right)_{exp} = \left(\frac{d\sigma}{d\Omega}\right)_{\text{Mott}} |F(q^2)|^2 \tag{10}$$

Nuclear Form Factors

- Now we have an equation that accounts for relativity, spin, and recoil off of a point mass.
- Nuclei are not point masses! How do we describe the structure inside of a nucleus?

$$\left(\frac{d\sigma}{d\Omega}\right)_{exp} = \left(\frac{d\sigma}{d\Omega}\right)_{\text{Mott}} |F(q^2)|^2 \tag{10}$$

- The term $|F(q^2)|^2$ is called a form factor. It contains all of the spatial and structural information about the target.
- If we assume the validity of the Born approximation (incident wave function $\approx$ scattered wave function) and no recoil the form factor can be written as a Fourier transform of the charge distribution.

Form Factors Cont.

$$F(q^2) = \int e^{\frac{iq\cdot x}{\hbar}} \rho(x) d^3x \xrightarrow{x \longrightarrow r} 4\pi \int \rho(r) \frac{sin\left(|q|r/\hbar\right)}{|q|r/\hbar} r^2 dr \tag{11}$$

Form Factors Cont.

$$F(q^2) = \int e^{\frac{iq\cdot x}{\hbar}} \rho(x) d^3x \xrightarrow{x \longrightarrow r} 4\pi \int \rho(r) \frac{sin\left(|q|r/\hbar\right)}{|q|r/\hbar} r^2 dr \qquad (11)$$

- This procedure can be inverted to find the charge distribution, ρ [1].

$$\rho(r) = \frac{1}{(2\pi)^3} \int F(q^2) e^{\frac{-iq\cdot x}{\hbar}} d^3q \qquad (12)$$

Form Factors Cont.

$$F(q^2) = \int e^{\frac{iq\cdot x}{\hbar}} \rho(x) d^3x \xrightarrow{x \longrightarrow r} 4\pi \int \rho(r) \frac{sin\left(|q|r/\hbar\right)}{|q|r/\hbar} r^2 dr \tag{11}$$

- This procedure can be inverted to find the charge distribution, ρ [1].

$$\rho(r) = \frac{1}{(2\pi)^3} \int F(q^2) e^{\frac{-iq\cdot x}{\hbar}} d^3q \tag{12}$$

- Let's approximate a nucleus as a hard sphere of charge.

Form Factors Cont.

$$F(q^2) = \int e^{\frac{iq\cdot x}{\hbar}} \rho(x) d^3x \xrightarrow{x \longrightarrow r} 4\pi \int \rho(r) \frac{\sin(|q|r/\hbar)}{|q|r/\hbar} r^2 dr \tag{11}$$

- This procedure can be inverted to find the charge distribution, ρ [1].

$$\rho(r) = \frac{1}{(2\pi)^3} \int F(q^2) e^{\frac{-iq\cdot x}{\hbar}} d^3q \tag{12}$$

- Let's approximate a nucleus as a hard sphere of charge.

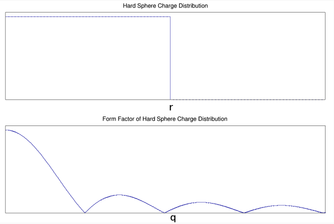

Figure 3: Hard Sphere Charge Distribution

Form Factors Cont.

$$F(q^2) = \int e^{\frac{iq\cdot x}{\hbar}} \rho(x) d^3x \xrightarrow{x \longrightarrow r} 4\pi \int \rho(r) \frac{sin\left(|q|r/\hbar\right)}{|q|r/\hbar} r^2 dr \qquad (11)$$

- This procedure can be inverted to find the charge distribution, ρ [1].

$$\rho(r) = \frac{1}{(2\pi)^3} \int F(q^2) e^{\frac{-iq\cdot x}{\hbar}} d^3q \qquad (12)$$

- Let's approximate a nucleus as a hard sphere of charge.

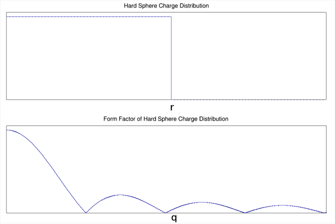

Figure 3: Hard Sphere Charge Distribution

- Yields oscillatory form factor.
- Charge radii can be estimated by minima location [1]!

$$R \approx \frac{4.5\hbar}{q} \qquad (13)$$

Charge Radius

- We can find charge radii by taking r$\rightarrow$0 in the form factor.
  - The wavelength of the electron, $\frac{\hbar}{q}$, is assumed to be much larger than the charge radius: $R \ll \frac{\hbar}{q} \implies \frac{Rq}{\hbar} \ll 1$.

Charge Radius

- We can find charge radii by taking r→0 in the form factor.
  - The wavelength of the electron, $\frac{\hbar}{q}$, is assumed to be much larger than the charge radius: $R \ll \frac{\hbar}{q} \implies \frac{Rq}{\hbar} \ll 1$.
- Next we apply the Euler formula to the form factor equation and Taylor expand the cosine term [1]:

$$F(q^2) = \int_0^\infty \int_{-1}^{1} \int_0^{2\pi} \rho(r) \left(1 - \frac{1}{2} \frac{|q||r| cos(\omega)}{\hbar}\right) r^2 d\phi \; dcos(\omega) \; dr \quad (14)$$

Charge Radius

- We can find charge radii by taking r→0 in the form factor.
  - The wavelength of the electron, $\frac{\hbar}{q}$, is assumed to be much larger than the charge radius: $R \ll \frac{\hbar}{q} \implies \frac{Rq}{\hbar} \ll 1$.
- Next we apply the Euler formula to the form factor equation and Taylor expand the cosine term [1]:

$$F(q^2) = \int_0^\infty \int_{-1}^1 \int_0^{2\pi} \rho(r) \left(1 - \frac{1}{2} \frac{|q||r|cos(\omega)}{\hbar}\right) r^2 d\phi \; dcos(\omega) \; dr \quad (14)$$

$$F(q^2) = 4\pi \int_0^\infty \rho(r) r^2 dr - 4\pi \frac{q^2}{6\hbar^2} \int_0^\infty \rho(r) r^4 dr \quad (15)$$

Charge Radius

- We can find charge radii by taking r→0 in the form factor.
  - The wavelength of the electron, $\frac{\hbar}{q}$, is assumed to be much larger than the charge radius: $R \ll \frac{\hbar}{q} \implies \frac{Rq}{\hbar} \ll 1$.
- Next we apply the Euler formula to the form factor equation and Taylor expand the cosine term [1]:

$$F(q^2) = \int_0^\infty \int_{-1}^1 \int_0^{2\pi} \rho(r) \left(1 - \frac{1}{2} \frac{|q||r|cos(\omega)}{\hbar}\right) r^2 d\phi \; dcos(\omega) \; dr \quad (14)$$

$$F(q^2) = 4\pi \int_0^\infty \rho(r) r^2 dr - 4\pi \frac{q^2}{6\hbar^2} \int_0^\infty \rho(r) r^4 dr \quad (15)$$

- Applying the normalization $4\pi \int_0^\infty \rho(r) r^2 dr = 1$, and defining the charge radius as $\langle r^2 \rangle = 4\pi \int_0^\infty r^2 \rho(r) r^2 dr$, we find:

Charge Radius

- We can find charge radii by taking $r \to 0$ in the form factor.
  - The wavelength of the electron, $\frac{\hbar}{q}$, is assumed to be much larger than the charge radius: $R \ll \frac{\hbar}{q} \implies \frac{Rq}{\hbar} \ll 1$.
- Next we apply the Euler formula to the form factor equation and Taylor expand the cosine term [1]:

$$F(q^2) = \int_0^\infty \int_{-1}^1 \int_0^{2\pi} \rho(r) \left(1 - \frac{1}{2}\frac{|q||r|cos(\omega)}{\hbar}\right) r^2 d\phi \; dcos(\omega) \; dr \quad (14)$$

$$F(q^2) = 4\pi \int_0^\infty \rho(r) r^2 dr - 4\pi \frac{q^2}{6\hbar^2} \int_0^\infty \rho(r) r^4 dr \quad (15)$$

- Applying the normalization $4\pi \int_0^\infty \rho(r) r^2 dr = 1$, and defining the charge radius as $\langle r^2 \rangle = 4\pi \int_0^\infty r^2 \rho(r) r^2 dr$, we find:

$$F(q^2) = 1 - \frac{q^2}{6\hbar^2}\langle r^2 \rangle \quad \to \quad \langle r^2 \rangle = -6\hbar^2 \frac{dF(q^2)}{dq^2}|_{q^2=0} \quad (16)$$

Rosenbluth Equation

- Now our cross section accounts for charge, relativity, spin, and recoil. Great! Is there anything still missing?

Rosenbluth Equation

- Now our cross section accounts for charge, relativity, spin, and recoil. Great! Is there anything still missing?
  - Magnetic interactions and internal structure are still not included.
  - Introduce a new magnetic term as was done for relativity [1].

Rosenbluth Equation

- Now our cross section accounts for charge, relativity, spin, and recoil. Great! Is there anything still missing?
  - Magnetic interactions and internal structure are still not included.
  - Introduce a new magnetic term as was done for relativity [1].

$$\left(\frac{d\sigma}{d\Omega}\right)_{\substack{\text{point}\\ \text{spin } 1/2}} = \left(\frac{d\sigma}{d\Omega}\right)_{Mott} \left(\left(1 - 2\tau \, tan^2\left(\frac{\theta}{2}\right)\right)\right), \quad \tau = \frac{Q^2}{4M} \tag{17}$$

Rosenbluth Equation

- Now our cross section accounts for charge, relativity, spin, and recoil. Great! Is there anything still missing?
  - Magnetic interactions and internal structure are still not included.
  - Introduce a new magnetic term as was done for relativity [1].

$$\left(\frac{d\sigma}{d\Omega}\right)_{\substack{\text{point}\\ \text{spin } 1/2}} = \left(\frac{d\sigma}{d\Omega}\right)_{Mott}\left(\left(1 - 2\tau\ tan^2\left(\frac{\theta}{2}\right)\right)\right), \quad \tau = \frac{Q^2}{4M} \qquad (17)$$

- Finally add in nuclear form factors to describe internal structure.

Rosenbluth Equation

- Now our cross section accounts for charge, relativity, spin, and recoil. Great! Is there anything still missing?
  - Magnetic interactions and internal structure are still not included.
  - Introduce a new magnetic term as was done for relativity [1].

$$\left(\frac{d\sigma}{d\Omega}\right)_{\substack{\text{point}\\ \text{spin } 1/2}} = \left(\frac{d\sigma}{d\Omega}\right)_{Mott}\left(\left(1 - 2\tau\ tan^2\left(\frac{\theta}{2}\right)\right)\right), \quad \tau = \frac{Q^2}{4M} \tag{17}$$

- Finally add in nuclear form factors to describe internal structure.

$$\left(\frac{d\sigma}{d\Omega}\right) = \left(\frac{d\sigma}{d\Omega}\right)_{Mott} * \left[\frac{G_E^2\left(Q^2\right) + \tau G_M^2\left(Q^2\right)}{1+\tau} + 2\tau G_M^2\left(Q^2\right) tan^2\left(\frac{\theta}{2}\right)\right] \tag{18}$$

Rosenbluth Equation

- Now our cross section accounts for charge, relativity, spin, and recoil. Great! Is there anything still missing?
  - Magnetic interactions and internal structure are still not included.
  - Introduce a new magnetic term as was done for relativity [1].

$$\left(\frac{d\sigma}{d\Omega}\right)_{\substack{\text{point}\\ \text{spin }1/2}} = \left(\frac{d\sigma}{d\Omega}\right)_{Mott} \left(\left(1 - 2\tau \; tan^2\left(\frac{\theta}{2}\right)\right)\right), \quad \tau = \frac{Q^2}{4M} \tag{17}$$

- Finally add in nuclear form factors to describe internal structure.

$$\left(\frac{d\sigma}{d\Omega}\right) = \left(\frac{d\sigma}{d\Omega}\right)_{Mott} * \left[\frac{G_E^2\left(Q^2\right) + \tau G_M^2\left(Q^2\right)}{1+\tau} + 2\tau G_M^2\left(Q^2\right) tan^2\left(\frac{\theta}{2}\right)\right] \tag{18}$$

$$G_E^p\left(Q^2=0\right) = 1 \;\; and \;\; G_M^p\left(Q^2=0\right) = 2.79 \tag{19}$$

$$G_E^n\left(Q^2=0\right) = 0 \;\; and \;\; G_M^n\left(Q^2=0\right) = -1.91 \tag{20}$$

Rosenbluth Equation Cont.

- G_E and G_M are known as the Sach's form factors. Several other form factors are commonly used.

Rosenbluth Equation Cont.

- G_E and G_M are known as the Sach's form factors. Several other form factors are commonly used.
  - F_1 and F_2 are called the Dirac and Pauli form factors respectively.

$$G_E\left(Q^2\right) = F_1\left(Q^2\right) - \mu\tau F_2\left(Q^2\right) \quad (21)$$

$$G_M\left(Q^2\right) = F_1\left(Q^2\right) + \mu F_2\left(Q^2\right) \quad (22)$$

Rosenbluth Equation Cont.

- G_E and G_M are known as the Sach's form factors. Several other form factors are commonly used.
  - F_1 and F_2 are called the Dirac and Pauli form factors respectively.

$$G_E\left(Q^2\right) = F_1\left(Q^2\right) - \mu\tau F_2\left(Q^2\right) \quad (21) \qquad G_M\left(Q^2\right) = F_1\left(Q^2\right) + \mu F_2\left(Q^2\right) \quad (22)$$

  - There are also the F_{ch} and F_m form factors used in this analysis.

$$F_{ch}\left(Q^2\right) = G_E\left(Q^2\right) \quad (23) \qquad F_m\left(Q^2\right) = \frac{G_M\left(Q^2\right)}{\mu} \quad (24)$$

Rosenbluth Equation Cont.

- G_E and G_M are known as the Sach's form factors. Several other form factors are commonly used.
  - F_1 and F_2 are called the Dirac and Pauli form factors respectively.

$$G_E\left(Q^2\right) = F_1\left(Q^2\right) - \mu\tau F_2\left(Q^2\right) \quad (21) \qquad G_M\left(Q^2\right) = F_1\left(Q^2\right) + \mu F_2\left(Q^2\right) \quad (22)$$

  - There are also the F_{ch} and F_m form factors used in this analysis.

$$F_{ch}\left(Q^2\right) = G_E\left(Q^2\right) \quad (23) \qquad F_m\left(Q^2\right) = \frac{G_M\left(Q^2\right)}{\mu} \quad (24)$$

- Now let's rewrite the cross section for the final Rosenbluth equation:

$$\left(\frac{d\sigma}{d\Omega}\right)_{exp} = \left(\frac{d\sigma}{d\Omega}\right)_{Mott} * \frac{1}{1+\tau}\left[G_E^2\left(Q^2\right) + \frac{\tau}{\epsilon} G_M^2\left(Q^2\right)\right] \quad (25)$$

$$\epsilon = \left(1 + 2(1+\tau) tan^2\left(\frac{\theta}{2}\right)\right)^{-1} \quad (26)$$

Experimental Setup

Experiment E08-014

- Experiment E08-014 ran in Jefferson Lab's Hall A in 2011 [2].
  - Measured inclusive cross sections of ^{2}H, ^{3}He, ^{4}He, ^{12}C, ^{40}Ca, and ^{48}Ca in the range of $1.1\ \mathrm{GeV/c} < Q^2 < 2.5\ \mathrm{GeV/c}$.
  - Compared heavy targets to two and three-nucleon targets to study short range correlations between two and three-nucleon clusters.

Experiment E08-014

- Experiment E08-014 ran in Jefferson Lab's Hall A in 2011 [2].
  - Measured inclusive cross sections of ^{2}H, ^{3}He, ^{4}He, ^{12}C, ^{40}Ca, and ^{48}Ca in the range of $1.1 \text{ GeV/c} < Q^2 < 2.5 \text{ GeV/c}$.
  - Compared heavy targets to two and three-nucleon targets to study short range correlations between two and three-nucleon clusters.
- E08-014 mostly took quasielastic data, but through a happy coincidence, KIN 3.2 was able to view the ^{3}He elastic peak.
  - $E_0 = 3.356$ GeV. Scattering angle of 20.51°.

Experiment E08-014

- Experiment E08-014 ran in Jefferson Lab's Hall A in 2011 [2].
  - Measured inclusive cross sections of ^{2}H, ^{3}He, ^{4}He, ^{12}C, ^{40}Ca, and ^{48}Ca in the range of 1.1 GeV/c $< Q^2 <$ 2.5 GeV/c.
  - Compared heavy targets to two and three-nucleon targets to study short range correlations between two and three-nucleon clusters.
- E08-014 mostly took quasielastic data, but through a happy coincidence, KIN 3.2 was able to view the ^{3}He elastic peak.
  - $E_0 = 3.356$ GeV. Scattering angle of 20.51°.

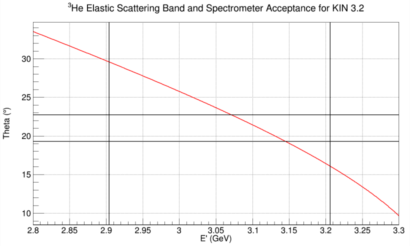

Figure 4: Elastic Band for ^{3}He.

Experiment E08-014

- Experiment E08-014 ran in Jefferson Lab's Hall A in 2011 [2].
  - Measured inclusive cross sections of ^{2}H, ^{3}He, ^{4}He, ^{12}C, ^{40}Ca, and ^{48}Ca in the range of 1.1 GeV/c $< Q^2 <$ 2.5 GeV/c.
  - Compared heavy targets to two and three-nucleon targets to study short range correlations between two and three-nucleon clusters.
- E08-014 mostly took quasielastic data, but through a happy coincidence, KIN 3.2 was able to view the ^{3}He elastic peak.
  - $E_0 = 3.356$ GeV. Scattering angle of 20.51°.

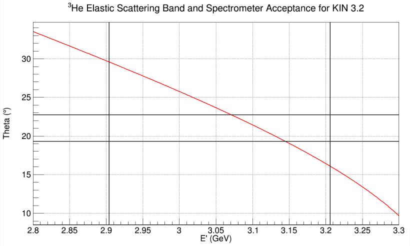

Figure 4: Elastic Band for ^{3}He.

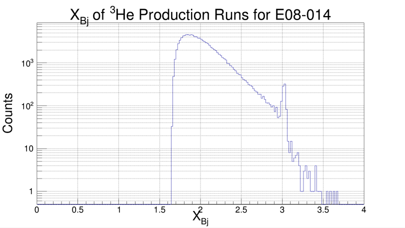

Figure 5: Elastic Peak in x_{Bj}.

- E08-014 used the standard Hall A configuration and detector packages.
  - Main trigger (S_1 & S_{2m} & GC).

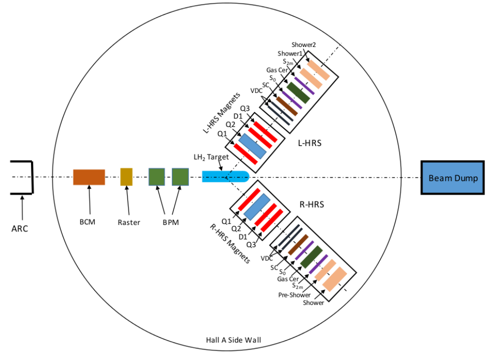

Figure 6: Hall A Top View. Standard Hall A configuration. Image from [3].

Cross Section Extraction

Extracting a Cross Section

- We can rewrite the cross section in a more useful form:

$$\left(\frac{d\sigma}{d\Omega}\right)_{exp} = \frac{ps * N_e}{N_{in} * \rho * LT * \epsilon_{det}} \frac{1}{\Delta\Omega \Delta P \Delta Z} \tag{27}$$

Extracting a Cross Section

- We can rewrite the cross section in a more useful form:

$$\left(\frac{d\sigma}{d\Omega}\right)_{exp} = \frac{ps * N_e}{N_{in} * \rho * LT * \epsilon_{det}} \frac{1}{\Delta\Omega\Delta P\Delta Z} \tag{27}$$

- Essentially, this is a game of electron counting.

Extracting a Cross Section

- We can rewrite the cross section in a more useful form:

$$\left(\frac{d\sigma}{d\Omega}\right)_{exp} = \frac{ps * N_e}{N_{in} * \rho * LT * \epsilon_{det}} \frac{1}{\Delta\Omega\Delta P\Delta Z} \tag{27}$$

- Essentially, this is a game of electron counting.
  - To count electrons we need the beam charge.

Extracting a Cross Section

- We can rewrite the cross section in a more useful form:

$$\left(\frac{d\sigma}{d\Omega}\right)_{exp} = \frac{ps * N_e}{N_{in} * \rho * LT * \epsilon_{det}} \frac{1}{\Delta\Omega\Delta P\Delta Z} \tag{27}$$

- Essentially, this is a game of electron counting.
  - To count electrons we need the beam charge.

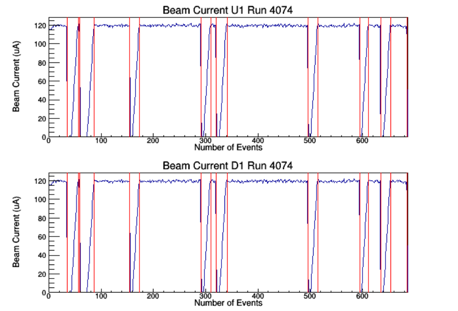

$$Q = \langle I_{beam} \rangle * time \tag{28}$$

$$N_{in} = \frac{Q}{e} \tag{29}$$

Particle Identification

- How many elastic electrons, N_e, were detected?
  - We need a pure electron sample. Pions can contaminate the sample.

Particle Identification

- How many elastic electrons, N_e, were detected?
  - We need a pure electron sample. Pions can contaminate the sample.
  - The EM calorimeters and GC can discriminate electrons from pions.

Particle Identification

- How many elastic electrons, N_e, were detected?
  - We need a pure electron sample. Pions can contaminate the sample.
  - The EM calorimeters and GC can discriminate electrons from pions.

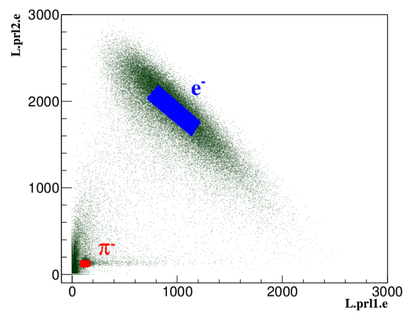

(a) Pion Rejectors

Figure 8: PID with the Pion Rejectors. Image from [2].

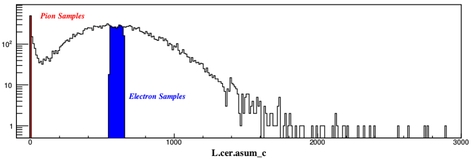

Figure 9: PID with the Gas Cherenkov. Image from [2].

Pion Rejectors PID

- For our six runs there appear to be very few pions.
- Some delta (knock-on) electrons are in the sample.
  - These delta electrons and few pions can be removed with a simple diagonal cut on the pion rejectors.

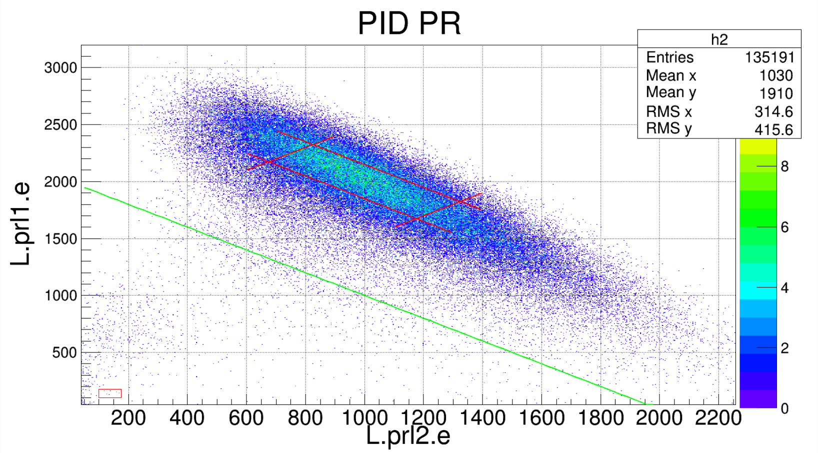

Gas Cherenkov PID

- Does the gas Cherenkov agree with the pion rejectors?

Gas Cherenkov PID

- Does the gas Cherenkov agree with the pion rejectors?
- Again there appear to be almost no pions at our kinematics.

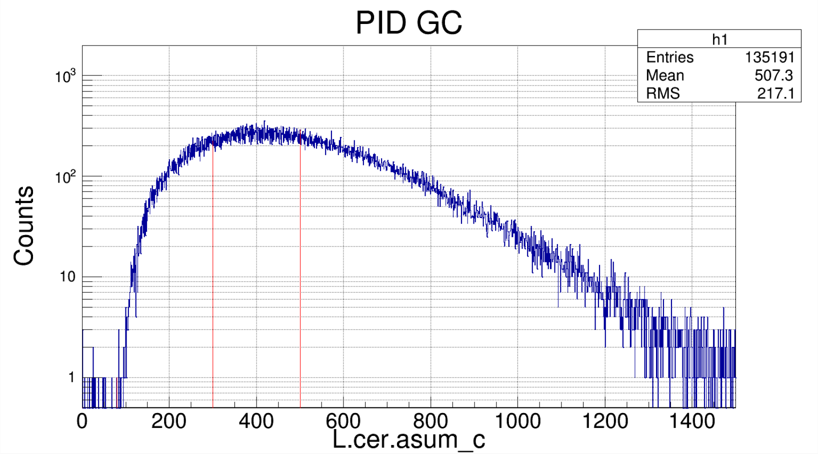

Figure 11: PID with the Gas Cherenkov.

Target Density

- Now we need to know how many scattering centers are in the target.

Target Density

- Now we need to know how many scattering centers are in the target.
- Let's look at the target's density profile to find ρ.

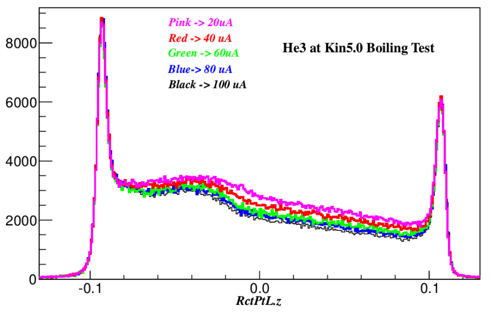

Figure 12: ^{3}**He Boiling Effect.** Image from [2].

Target Density

- Now we need to know how many scattering centers are in the target.
- Let's look at the target's density profile to find ρ.

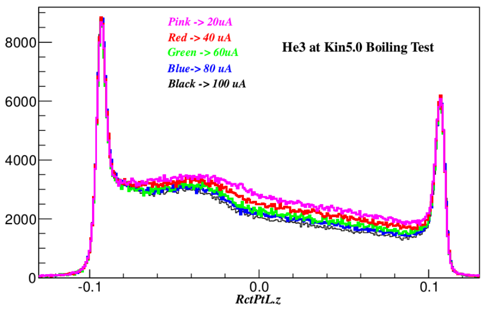

Figure 12: ^{3}**He Boiling Effect.** Image from [2].

- The density is not constant along the cell due to boiling effects.
- CFD calculations by Silviu Covrig allowed ρ to be calculated [4].
  - $0.013\ \mathrm{g/cm^3} \pm 0.0004\ \mathrm{g/cm^3}$.

Simulating Elastic Electrons

- How do we know how many events were elastic?

Simulating Elastic Electrons

- How do we know how many events were elastic?
  - Find the elastic electron yield.
  - Count electrons in the elastic peak ($X_{Bj} = 3$).

Simulating Elastic Electrons

- How do we know how many events were elastic?
  - Find the elastic electron yield.
  - Count electrons in the elastic peak ($X_{Bj} = 3$).
- Before finding the experimental elastic electron yield we want a point of comparison.

Simulating Elastic Electrons

- How do we know how many events were elastic?
  - Find the elastic electron yield.
  - Count electrons in the elastic peak ($X_{Bj} = 3$).
- Before finding the experimental elastic electron yield we want a point of comparison.
  - We can simulate what the elastic electron spectrum is expected to look like at our kinematics using SIMC.

Simulating Elastic Electrons

- How do we know how many events were elastic?
  - Find the elastic electron yield.
  - Count electrons in the elastic peak ($X_{Bj} = 3$).
- Before finding the experimental elastic electron yield we want a point of comparison.
  - We can simulate what the elastic electron spectrum is expected to look like at our kinematics using SIMC.
- SIMC:
  - Monte Carlo generates events randomly in given kinematic ranges.
  - Transports electrons from scattering vertex through spectrometers to detector stack.
  - Contains old ^{3}He elastic scattering model from Amroun *et al* [5].
  - Shape of form factors and cross section should be accurate.
  - Cross section magnitude is expected to be off at our kinematics.
  - Can calculate radiative effects.

SIMC Output

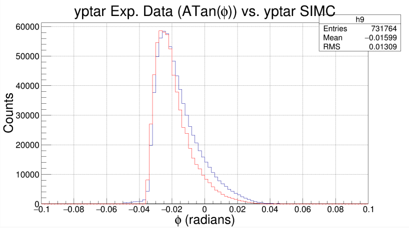

Figure 13: ϕ**.** In plane angle.

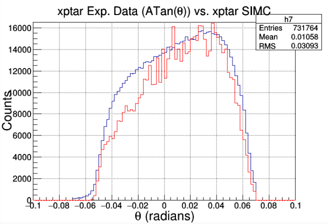

Figure 14: θ**.** Out of plane angle.

- Red is SIMC and blue is data.
- ϕ and θ both look decent.
- There is a shift in dP.
  - Known issue with SIMC.
  - Little impact on final measurement.

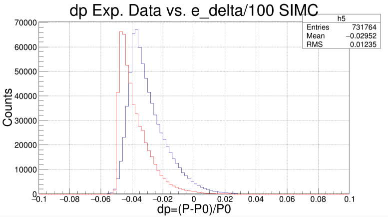

Figure 15: **dP** Momentum fraction.

Aluminium Background Subtraction

- Take a closer look at the X_{Bj} plot from earlier (blue histogram).
  - What are the events above the ^{3}He elastic peak?

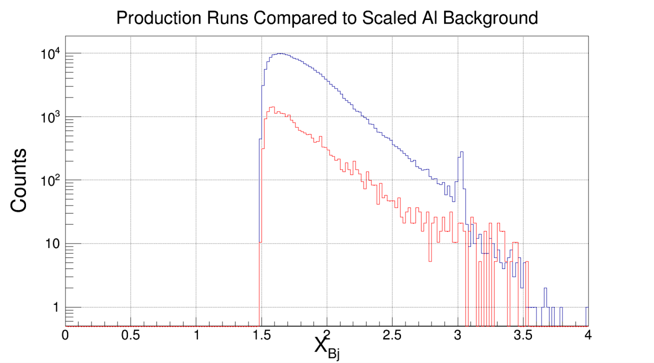

Figure 16: Scaled Aluminium Background and X_{Bj}.

Aluminium Background Subtraction

- Take a closer look at the X_{Bj} plot from earlier (blue histogram).
  - What are the events above the ^{3}He elastic peak?

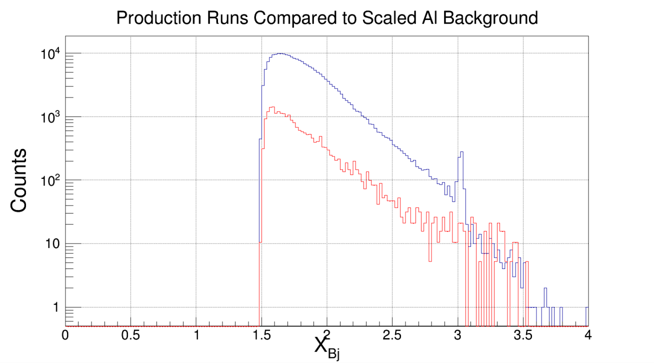

Figure 16: Scaled Aluminium Background and X_{Bj}.

- Aluminium contamination from target cell (red histogram).
  - Use dummy cell to subtract Al events.
  - Scale dummy by charge, thickness, and radiative corrections.

Aluminium Background Subtraction Cont.

- What happens when we subtract off the aluminium contamination from the X_{Bj} spectrum?

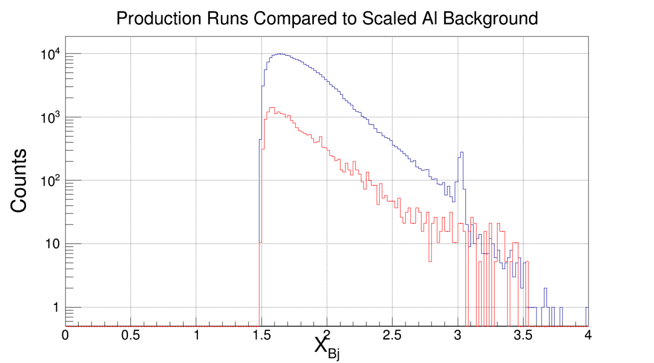

Figure 17: Scaled Aluminium Background and X_{Bj}.

Aluminium Background Subtraction Cont.

- What happens when we subtract off the aluminium contamination from the X_{Bj} spectrum?

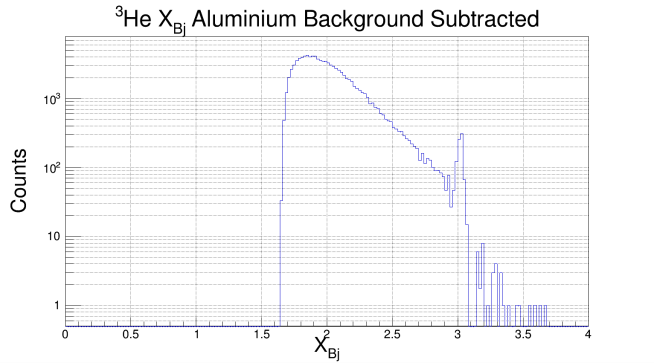

Figure 18: Aluminium Subtracted X_{Bj}.

- Now most of the events above the elastic peak disappear!

Fitting the Elastic Peak

- How do we count the number of electrons in the elastic peak, N_e?

Fitting the Elastic Peak

- How do we count the number of electrons in the elastic peak, N_e?
  - Fit the peak and integrate over the elastic peak.

Fitting the Elastic Peak

- How do we count the number of electrons in the elastic peak, N_e?
  - Fit the peak and integrate over the elastic peak.
- What kind of fit might be appropriate?

Fitting the Elastic Peak

- How do we count the number of electrons in the elastic peak, N_e?
  - Fit the peak and integrate over the elastic peak.
- What kind of fit might be appropriate?
  - QE background looks exponential and elastic peak looks Gaussian.
  - Create a fit equation summing an exponential and a Gaussian:

Fitting the Elastic Peak

- How do we count the number of electrons in the elastic peak, N_e?
  - Fit the peak and integrate over the elastic peak.
- What kind of fit might be appropriate?
  - QE background looks exponential and elastic peak looks Gaussian.
  - Create a fit equation summing an exponential and a Gaussian:

$$F_{combined} = e^{(P_0+P_1*x)} + P_2 * e^{\left(\frac{-1}{2}\left(\frac{x-P_3}{P_4}\right)^2\right)} \tag{30}$$

Fitting the Elastic Peak

- How do we count the number of electrons in the elastic peak, N_e?
  - Fit the peak and integrate over the elastic peak.
- What kind of fit might be appropriate?
  - QE background looks exponential and elastic peak looks Gaussian.
  - Create a fit equation summing an exponential and a Gaussian:

$$F_{combined} = e^{(P_0+P_1*x)} + P_2 * e^{\left(\frac{-1}{2}\left(\frac{x-P_3}{P_4}\right)^2\right)} \tag{30}$$

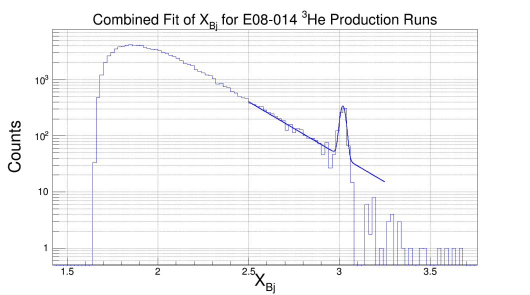

Figure 19: Combined Fit of X_{Bj} for E08-014.

Comparing SIMC and Experimental Yields

- Now let's look at the elastics from SIMC.

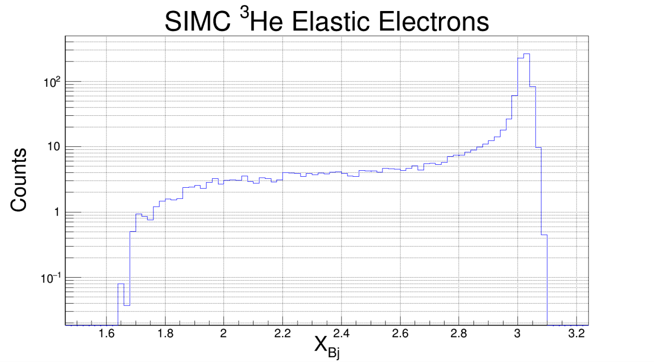

Figure 20: SIMC Elastically Scattered Electrons.

Comparing SIMC and Experimental Yields

- Now let's look at the elastics from SIMC.

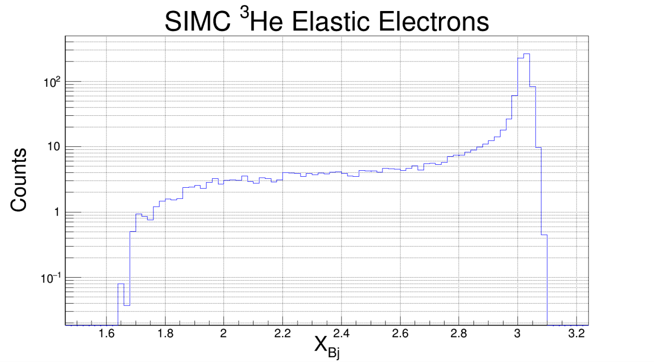

Figure 20: SIMC Elastically Scattered Electrons.

- The spectrum looks reasonable.
  - Prominent elastic peak at $X_{Bj} = 3$.
  - Nice radiative tail as expected.

Comparing SIMC and Experimental Yields Cont.

- How do we compare simulated elastic events to experimental events that are mostly quasielastic?

Comparing SIMC and Experimental Yields Cont.

- How do we compare simulated elastic events to experimental events that are mostly quasielastic?
  - We can fit only the QE background and then sum the fit with the SIMC elastics.
  - The QE fit is made in the region where few elastics are expected.

Comparing SIMC and Experimental Yields Cont.

- How do we compare simulated elastic events to experimental events that are mostly quasielastic?
  - We can fit only the QE background and then sum the fit with the SIMC elastics.
  - The QE fit is made in the region where few elastics are expected.

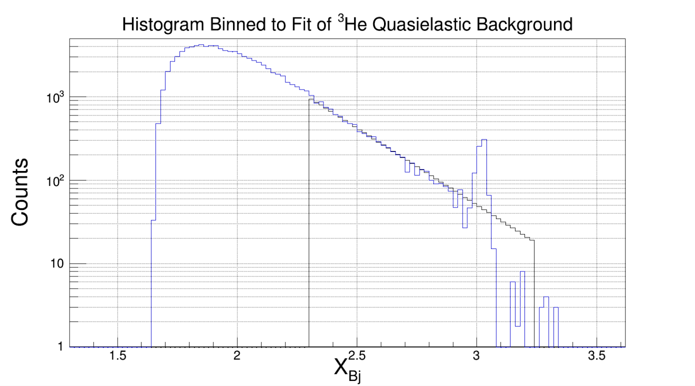

Figure 21: Histogram Binned to Fit of Quasielastic Background.

Comparing SIMC and Experimental Yields Cont.

- Finally we can compare the elastic electron yield from SIMC and experimental data.

Comparing SIMC and Experimental Yields Cont.

- Finally we can compare the elastic electron yield from SIMC and experimental data.
  - The area under the Gaussian of the two combined fits, but above the QE background, represents the elastic electron yield.
  - The elastic electron yield is directly proportional to the cross section.

Comparing SIMC and Experimental Yields Cont.

- Finally we can compare the elastic electron yield from SIMC and experimental data.
  - The area under the Gaussian of the two combined fits, but above the QE background, represents the elastic electron yield.
  - The elastic electron yield is directly proportional to the cross section.
  - Note that the real data yield is increased slightly to correct for live-time and various efficiencies.

Comparing SIMC and Experimental Yields Cont.

- Finally we can compare the elastic electron yield from SIMC and experimental data.
  - The area under the Gaussian of the two combined fits, but above the QE background, represents the elastic electron yield.
  - The elastic electron yield is directly proportional to the cross section.
  - Note that the real data yield is increased slightly to correct for live-time and various efficiencies.
- Recall that at our kinematics the old ^{3}He model in SIMC has the correct cross section shape but incorrect magnitude [5].
- SIMC produces the average cross section for this experiment based on the previous model.

Comparing SIMC and Experimental Yields Cont.

- Finally we can compare the elastic electron yield from SIMC and experimental data.
  - The area under the Gaussian of the two combined fits, but above the QE background, represents the elastic electron yield.
  - The elastic electron yield is directly proportional to the cross section.
  - Note that the real data yield is increased slightly to correct for live-time and various efficiencies.
- Recall that at our kinematics the old ^{3}He model in SIMC has the correct cross section shape but incorrect magnitude [5].
- SIMC produces the average cross section for this experiment based on the previous model.
- If the SIMC cross section is scaled by a constant until the SIMC yield matches the experimental yield then the average cross section SIMC produces will equal the experimental cross section.

Cross Section Value

- Yields plots for the experimental data and SIMC scaled to match.
  - Red is SIMC + QE background fit and blue is experimental data.

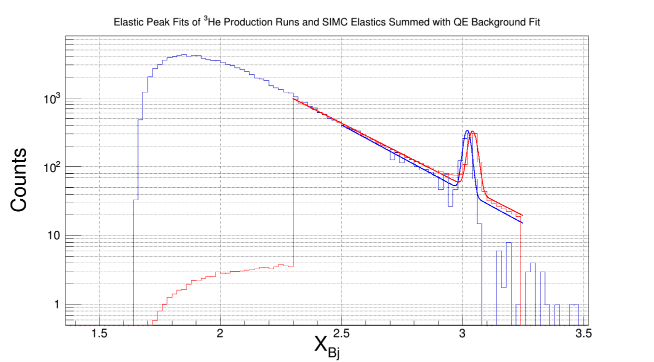

Figure 22: SIMC + QE Scaled to Experimental Elastic Electron Yield.

Cross Section Value

- Yields plots for the experimental data and SIMC scaled to match.
  - Red is SIMC + QE background fit and blue is experimental data.

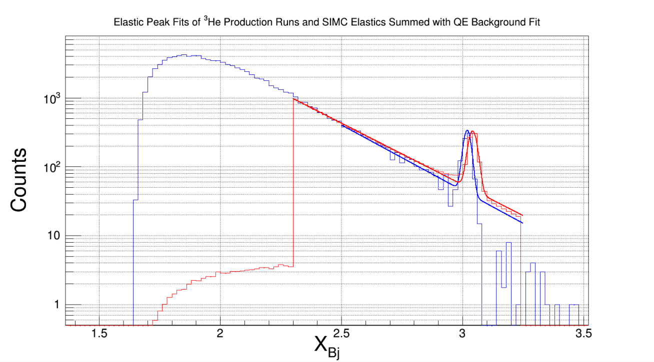

Figure 22: SIMC + QE Scaled to Experimental Elastic Electron Yield.

- Yield shapes are similar. Slight shift is likely a Z offset issue.
- SIMC scale factor to match data = 1.01984.
- New ^{3}He cross section value is $1.335 * 10^{-10}$ fm^{-2}/sr.

Where to Place the Data Point

- We now have the cross section's magnitude. Great! We're done right?

Where to Place the Data Point

- We now have the cross section's magnitude. Great! We're done right?
  - Wrong!

Where to Place the Data Point

- We now have the cross section's magnitude. Great! We're done right?
  - Wrong!
  - Where do we put our point?
  - What is the uncertainty?

Where to Place the Data Point

- We now have the cross section's magnitude. Great! We're done right?
  - Wrong!
  - Where do we put our point?
  - What is the uncertainty?
- Can't we just calculate Q^2 from the center of our bin and be done?
- The bin center is only correct if the function is linear [6].

Where to Place the Data Point

- We now have the cross section's magnitude. Great! We're done right?
  - Wrong!
  - Where do we put our point?
  - What is the uncertainty?
- Can't we just calculate Q^2 from the center of our bin and be done?
- The bin center is only correct if the function is linear [6].

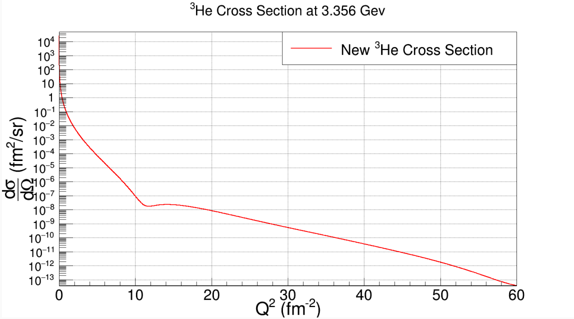

Figure 23: ^{3}He Elastic Cross Section at 3.356 GeV.

Where to Place the Data Point Cont.

- Now let's zoom in and remove the log scale to see the true shape.

Where to Place the Data Point Cont.

- Now let's zoom in and remove the log scale to see the true shape.

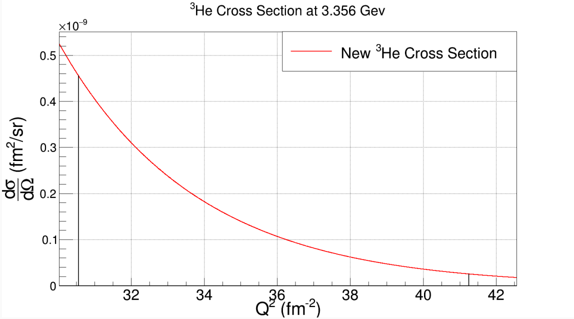

Figure 24: ^{3}He Elastic Cross Section Q^2 Bin at 3.356 GeV.

Where to Place the Data Point Cont.

- Now let's zoom in and remove the log scale to see the true shape.

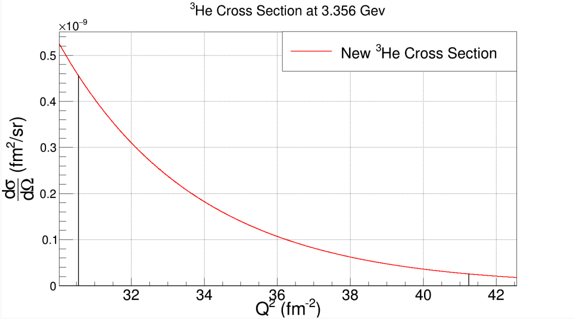

Figure 24: ^{3}He Elastic Cross Section Q^2 Bin at 3.356 GeV.

- Clearly not linear.
- Weight the Q^2 values in the bin by the cross section magnitude.

Where to Place the Data Point Cont.

- Now let's zoom in and remove the log scale to see the true shape.

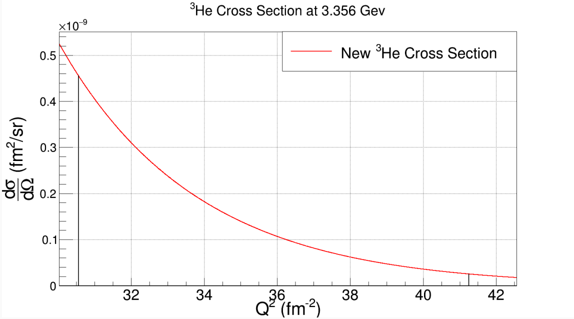

Figure 24: ^{3}He Elastic Cross Section Q^2 Bin at 3.356 GeV.

- Clearly not linear.
- Weight the Q^2 values in the bin by the cross section magnitude.
- The bin center would place the Q^2 at 35.90 fm^{-2}.
- The weighted bin center is at $Q^2 = 34.19$ fm^{-2}.

Uncertainty

- Lastly, we need to quantify the uncertainty on our point.

Uncertainty Source	Cross Section Uncertainty
Statistical Sources	
Electron Yield	4.21%
Al Background Subtraction	1.1%
Total Statistical	**4.36%**
Systematic Sources	
Target Density	3.08%
Optics Calibration	2.248%
GC Efficiency	1.32%
Beam/Target Offsets	1.1%
Radiative Corrections	1%
Beam Charge	1%
VDC Single-Track Efficiency	1%
Trigger Efficiency	1%
Beam Energy	0.72%
SIMC Model Comparison to Reality	0.5%
PR Cut	0.055%
Y_{target} Position	0.045%
Live-time	0.01145%
Total Systematic	**4.72%**
Total Uncertainty Statistical & Systematic	**6.42%**

Comparison to Other Measurements

- Our cross section measurement is now $1.335 \pm 0.086 * 10^{-6}$ μb/sr at $Q^2 = 34.19$ fm^{-2}.

Comparison to Other Measurements

- Our cross section measurement is now $1.335 \pm 0.086 * 10^{-6}$ μb/sr at $Q^2 = 34.19$ fm^{-2}.
- JLab took high Q^2 data for ^{3}He [7].
  - $E_0 = 3.304$ GeV. Scattering angle of 20.83°.
  - Cross section $= 1.57 \pm 0.10 * 10^{-6}$ μb/sr at $Q^2 = 34.1$ fm^{-2}.
  - This analysis' cross section is $\approx$ 15% smaller.
  - Accounting for our higher Q^2 the error bars should nearly overlap.

Comparison to Other Measurements

- Our cross section measurement is now $1.335 \pm 0.086 * 10^{-6}\ \mu b/sr$ at $Q^2 = 34.19\ fm^{-2}$.
- JLab took high Q^2 data for ^3He [7].
  - $E_0 = 3.304$ GeV. Scattering angle of 20.83°.
  - Cross section $= 1.57 \pm 0.10 * 10^{-6}\ \mu b/sr$ at $Q^2 = 34.1\ fm^{-2}$.
  - This analysis' cross section is $\approx$ 15% smaller.
  - Accounting for our higher Q^2 the error bars should nearly overlap.
- Cross section estimate from older SIMC model [5].
  - $E_0 = 3.356$ GeV. Scattering angle of 20.51°.
  - Cross section $= 1.887 * 10^{-6}\ \mu b/sr$ at $Q^2 = 34.19\ fm^{-2}$.
  - This analysis' cross section is $\approx$ 30% smaller.
  - Old model had very little high Q^2 data so we expect the magnitude to not be extremely accurate.

Comparison to Other Measurements

- Our cross section measurement is now $1.335 \pm 0.086 * 10^{-6}$ μb/sr at $Q^2 = 34.19$ fm^{-2}.
- JLab took high Q^2 data for ^{3}He [7].
  - $E_0 = 3.304$ GeV. Scattering angle of 20.83°.
  - Cross section = $1.57 \pm 0.10 * 10^{-6}$ μb/sr at $Q^2 = 34.1$ fm^{-2}.
  - This analysis' cross section is $\approx$ 15% smaller.
  - Accounting for our higher Q^2 the error bars should nearly overlap.
- Cross section estimate from older SIMC model [5].
  - $E_0 = 3.356$ GeV. Scattering angle of 20.51°.
  - Cross section = $1.887 * 10^{-6}$ μb/sr at $Q^2 = 34.19$ fm^{-2}.
  - This analysis' cross section is $\approx$ 30% smaller.
  - Old model had very little high Q^2 data so we expect the magnitude to not be extremely accurate.
- In sum this new point seems reasonably consistent with other data.

Global Fits

World Data

- We now have a new cross section!

World Data

- We now have a new cross section! But what use is a single point?

World Data

- We now have a new cross section! But what use is a single point?
- We need context to learn anything.

World Data

- We now have a new cross section! But what use is a single point?
- We need context to learn anything.
- For context we can gather the world data for ^{3}He elastic cross sections.
  - We can also gather the ^{3}H world data so we have mirror nuclei.
  - The world data for ^{3}H and ^{3}He stretches back over 50 years!
  - Experiments were done at at least nine different facilities.
  - Many experiments used different methodologies.

World Data

- We now have a new cross section! But what use is a single point?
- We need context to learn anything.
- For context we can gather the world data for ^{3}He elastic cross sections.
  - We can also gather the ^{3}H world data so we have mirror nuclei.
  - The world data for ^{3}H and ^{3}He stretches back over 50 years!
  - Experiments were done at at least nine different facilities.
  - Many experiments used different methodologies.
- This analysis used as many of the data sets as possible.
  - Some papers did not publish their data.
  - Some published only form factors and/or did not publish scattering angles and energies.
- This analysis adds new JLab high Q^2 data for ^{3}He as well as the new cross section from SRC $X>2$.

Sum of Gaussians Parametrization

- What do we want to get out of the world data?

Sum of Gaussians Parametrization

- What do we want to get out of the world data?
  - Form factors, charge densities, and charge radii.

Sum of Gaussians Parametrization

- What do we want to get out of the world data?
  - Form factors, charge densities, and charge radii.
- How do we find these quantities?

Sum of Gaussians Parametrization

- What do we want to get out of the world data?
  - Form factors, charge densities, and charge radii.
- How do we find these quantities?
  - We need some parametrization to fit the world data.

Sum of Gaussians Parametrization

- What do we want to get out of the world data?
  - Form factors, charge densities, and charge radii.
- How do we find these quantities?
  - We need some parametrization to fit the world data.
- Select a sum of Gaussians (SOG) parametrization [8].

Sum of Gaussians Parametrization

- What do we want to get out of the world data?
  - Form factors, charge densities, and charge radii.
- How do we find these quantities?
  - We need some parametrization to fit the world data.
- Select a sum of Gaussians (SOG) parametrization [8].
  - Parametrizes form factors using multiple Gaussians placed at different radii.
  - Disallows unphysically small structures in the charge density.
  - q_{max} based on limited data: $\lambda = \frac{2\pi}{q_{max}}$.

Sum of Gaussians Parametrization

- What do we want to get out of the world data?
  - Form factors, charge densities, and charge radii.
- How do we find these quantities?
  - We need some parametrization to fit the world data.
- Select a sum of Gaussians (SOG) parametrization [8].
  - Parametrizes form factors using multiple Gaussians placed at different radii.
  - Disallows unphysically small structures in the charge density.
  - q_{max} based on limited data: $\lambda = \frac{2\pi}{q_{max}}$.

$$\rho(r) = \frac{Ze}{2\pi^{3/2}\gamma^3} \sum_{i=1}^{N} \frac{Q_i}{1 + \frac{2R_i^2}{\gamma^2}} \left(e^{-(r-R_i)^2/\gamma^2} + e^{-(r+R_i)^2/\gamma^2} \right) \tag{31}$$

- With normalization:

$$4\pi \int_0^\infty \rho(r) r^2 dr = Ze \tag{32}$$

SOG Cont.

- When using the plane wave born approximation the form factors can be written as [8]:

$$F_{(ch,m)}(q) = exp\left(-\frac{1}{4}q^2\gamma^2\right)\sum_{i=1}^{N}\frac{Q_{i(ch,m)}}{1+2R_i^2/\gamma^2}\left(\cos(qR_i)+\frac{2R_i^2}{\gamma^2}\frac{\sin(qR_i)}{qR_i}\right) \tag{33}$$

SOG Cont.

- When using the plane wave born approximation the form factors can be written as [8]:

$$F_{(ch,m)}(q) = exp\left(-\frac{1}{4}q^2\gamma^2\right)\sum_{i=1}^{N}\frac{Q_{i(ch,m)}}{1+2R_i^2/\gamma^2}\left(\cos(qR_i)+\frac{2R_i^2}{\gamma^2}\frac{\sin(qR_i)}{qR_i}\right) \tag{33}$$

- The Q_i are the fit parameters.
  - Represent the fraction of charge held by each Gaussian.
  - $Q_i > 0$ and $\sum Q_i = 1$.

SOG Cont.

- When using the plane wave born approximation the form factors can be written as [8]:

$$F_{(ch,m)}(q) = exp\left(-\frac{1}{4}q^2\gamma^2\right)\sum_{i=1}^{N}\frac{Q_{i(ch,m)}}{1+2R_i^2/\gamma^2}\left(\cos(qR_i)+\frac{2R_i^2}{\gamma^2}\frac{\sin(qR_i)}{qR_i}\right) \tag{33}$$

- The Q_i are the fit parameters.
  - Represent the fraction of charge held by each Gaussian.
  - $Q_i > 0$ and $\sum Q_i = 1$.
- The R_i represent the radii at which each Gaussian is placed.
  - Selected pseudorandomly then optimized.

SOG Cont.

- When using the plane wave born approximation the form factors can be written as [8]:

$$F_{(ch,m)}(q) = exp\left(-\frac{1}{4}q^2\gamma^2\right)\sum_{i=1}^{N}\frac{Q_{i(ch,m)}}{1+2R_i^2/\gamma^2}\left(\cos(qR_i)+\frac{2R_i^2}{\gamma^2}\frac{\sin(qR_i)}{qR_i}\right) \tag{33}$$

- The Q_i are the fit parameters.
  - Represent the fraction of charge held by each Gaussian.
  - $Q_i > 0$ and $\sum Q_i = 1$.
- The R_i represent the radii at which each Gaussian is placed.
  - Selected pseudorandomly then optimized.
- The differential cross section can be written as [5]:

$$\frac{d\sigma}{d\Omega} = \left(\frac{d\sigma}{d\Omega}\right)_{Mott}\frac{1}{\eta}\left[\frac{q^2}{\mathbf{q}^2}F_{ch}^2(q)+\frac{\mu^2 q^2}{2M^2}\left(\frac{1}{2}\frac{q^2}{\mathbf{q}^2}+\tan^2\left(\frac{\theta}{2}\right)\right)F_m^2(q)\right] \tag{34}$$

$$\eta = 1 + q^2/4M^2 \tag{35}$$

SOG Cont.

- To account for the Born approximation we utilize Q_{eff} in place of a full phase shift code.

$$Q_{eff}^2 = Q^2 \left(1 + \frac{1.5Z\alpha}{E_0 * 1.12 * A^{\frac{1}{3}}}\right)^2 \tag{36}$$

SOG Cont.

- To account for the Born approximation we utilize Q_{eff} in place of a full phase shift code.

$$Q_{eff}^2 = Q^2 \left(1 + \frac{1.5Z\alpha}{E_0 * 1.12 * A^{\frac{1}{3}}}\right)^2 \tag{36}$$

- Next we need to decide how to generate our starting radii, R_i.

SOG Cont.

- To account for the Born approximation we utilize Q_{eff} in place of a full phase shift code.

$$Q_{eff}^2 = Q^2 \left(1 + \frac{1.5 Z\alpha}{E_0 * 1.12 * A^{\frac{1}{3}}}\right)^2 \tag{36}$$

- Next we need to decide how to generate our starting radii, R_i.
  - There is an R_{max} beyond which there is almost no charge density.
  - $R_{max} \approx 5$ fm for our nuclei.
  - Consecutive R_i spacing is closer at smaller radii.
  - $R_i < R_{max}/2 \approx$ half as far apart as spacing of $R_i > R_{max}/2$.

SOG Cont.

- To account for the Born approximation we utilize Q_{eff} in place of a full phase shift code.

$$Q_{eff}^2 = Q^2 \left(1 + \frac{1.5 Z\alpha}{E_0 * 1.12 * A^{\frac{1}{3}}}\right)^2 \tag{36}$$

- Next we need to decide how to generate our starting radii, R_i.
  - There is an R_{max} beyond which there is almost no charge density.
  - $R_{max} \approx 5$ fm for our nuclei.
  - Consecutive R_i spacing is closer at smaller radii.
  - $R_i < R_{max}/2 \approx$ half as far apart as spacing of $R_i > R_{max}/2$.
- Essentially, the set of R_i constitute a model of the charge distribution.
- R_i are generated within pseudorandom ranges initially to span the model space.
- R_i are then adjusted up and down by 0.1 fm until χ^2 is minimized.

Selecting the Number of Gaussians

- How do we select how many Gaussians, N_{Gaus}, to use in our fit?

Selecting the Number of Gaussians

- How do we select how many Gaussians, N_{Gaus}, to use in our fit?
  - χ^2 is useful, but it can be misleading. Reduced χ^2 can help.

$$\chi^2 = \sum_{n=1}^{N} \frac{(\sigma_{exp} - \sigma_{fit})^2}{\Delta^2} \tag{37}$$

$$r\chi^2 = \frac{\chi^2}{N - N_{var} - 1} \tag{38}$$

Selecting the Number of Gaussians

- How do we select how many Gaussians, N_{Gaus}, to use in our fit?
  - χ^2 is useful, but it can be misleading. Reduced χ^2 can help.

$$\chi^2 = \sum_{n=1}^{N} \frac{\left(\sigma_{exp} - \sigma_{fit}\right)^2}{\Delta^2} \quad (37) \qquad r\chi^2 = \frac{\chi^2}{N - N_{var} - 1} \quad (38)$$

- Akaike and Bayesian information criterion are more powerful [9].

$$AIC = N \ln\left(\frac{\chi^2}{N}\right) + 2N_{var} \quad (39) \qquad BIC = N \ln\left(\frac{\chi^2}{N}\right) + \ln(N)\, N_{var} \quad (40)$$

Selecting the Number of Gaussians

- How do we select how many Gaussians, N_{Gaus}, to use in our fit?
  - χ^2 is useful, but it can be misleading. Reduced χ^2 can help.

$$\chi^2 = \sum_{n=1}^{N} \frac{(\sigma_{exp} - \sigma_{fit})^2}{\Delta^2} \quad (37) \qquad r\chi^2 = \frac{\chi^2}{N - N_{var} - 1} \quad (38)$$

- Akaike and Bayesian information criterion are more powerful [9].

$$AIC = N \ln\left(\frac{\chi^2}{N}\right) + 2N_{var} \quad (39) \qquad BIC = N \ln\left(\frac{\chi^2}{N}\right) + \ln(N)\, N_{var} \quad (40)$$

- The Q_i are not forced to sum to unity.
  - By not forcing $\sum Q_i = 1$ the $\sum Q_i$ becomes a measure of how well our fit and the current data approach physical requirements.

Selecting the Number of Gaussians

- How do we select how many Gaussians, N_{Gaus}, to use in our fit?
  - χ^2 is useful, but it can be misleading. Reduced χ^2 can help.

$$\chi^2 = \sum_{n=1}^{N} \frac{(\sigma_{exp} - \sigma_{fit})^2}{\Delta^2} \qquad (37) \qquad\qquad r\chi^2 = \frac{\chi^2}{N - N_{var} - 1} \qquad (38)$$

- Akaike and Bayesian information criterion are more powerful [9].

$$AIC = N \ln\left(\frac{\chi^2}{N}\right) + 2N_{var} \quad (39) \qquad BIC = N \ln\left(\frac{\chi^2}{N}\right) + \ln(N)\, N_{var} \quad (40)$$

- The Q_i are not forced to sum to unity.
  - By not forcing $\sum Q_i = 1$ the $\sum Q_i$ becomes a measure of how well our fit and the current data approach physical requirements.
- Lastly the fits can be visually inspected for physicality.

Selecting the Number of Gaussians Cont.

- Compare the metrics for different values of N_{Gaus} for ^{3}He and ^{3}H.

Selecting the Number of Gaussians Cont.

- Compare the metrics for different values of N_{Gaus} for ^{3}He and ^{3}H.

$\mathbf{N}_{Gaus}$	**Avg.** χ^2	**r**χ^2	**BIC**	**AIC**	$\sum \mathbf{Q}_{i_{ch}}$	$\sum \mathbf{Q}_{i_m}$	χ^2_{max}	**'Good' Fits**
8	584.902	2.41695	255.440	223.228	**1.00769**	1.11065	765	11
9	470.435	1.96014	204.590	172.375	1.00851	**1.02161**	521	58
10	469.177	1.97133	209.454	173.793	1.00812	1.08196	519	66
11	445.136	1.88617	**201.387**	162.233	1.00843	1.04007	503	67
12	**436.264**	**1.86438**	201.727	**159.045**	1.00839	1.02557	501	**75**
13	439.084	1.89260	208.924	162.685	1.00947	1.03975	500	56

Table 2: Determination of N_{Gaus} for ^{3}He

Selecting the Number of Gaussians Cont.

- Compare the metrics for different values of N_{Gaus} for ^{3}He and ^{3}H.

N_{Gaus}	Avg. χ^2	$r\chi^2$	BIC	AIC	$\sum Q_{i_{ch}}$	$\sum Q_{i_m}$	χ^2_{max}	'Good' Fits
8	584.902	2.41695	255.440	223.228	**1.00769**	1.11065	765	11
9	470.435	1.96014	204.590	172.375	1.00851	**1.02161**	521	58
10	469.177	1.97133	209.454	173.793	1.00812	1.08196	519	66
11	445.136	1.88617	**201.387**	162.233	1.00843	1.04007	503	67
12	**436.264**	**1.86438**	201.727	**159.045**	1.00839	1.02557	501	**75**
13	439.084	1.89260	208.924	162.685	1.00947	1.03975	500	56

Table 2: Determination of N_{Gaus} for ^{3}He

N_{Gaus}	Avg. χ^2	$r\chi^2$	BIC	AIC	$\sum Q_{i_{ch}}$	$\sum Q_{i_m}$	χ^2_{max}	'Good' Fits
7	611.690	2.79310	**263.039**	238.851	**1.08373**	1.32730	611.7	1
8 close	601.836	2.77344	264.694	237.051	1.09013	1.32859	603	32
8 wide	601.752	2.79892	264.661	**237.018**	1.08970	1.33270	603	39
9	601.768	2.82579	270.123	239.025	1.08849	1.31982	604	**95**
10	601.893	2.84416	275.627	241.074	1.09248	**1.29611**	603	78
11	**600.750**	**2.77305**	280.637	242.629	1.08699	1.34100	602	88

Table 3: Determination of N_{Gaus} for ^{3}H

^{3}He Fits

- Let's look at the $N_{Gaus} = 12$ ^{3}He form factor plots.

^{3}He Fits

- Let's look at the N$_{Gaus}$ = 12 ^{3}He form factor plots.

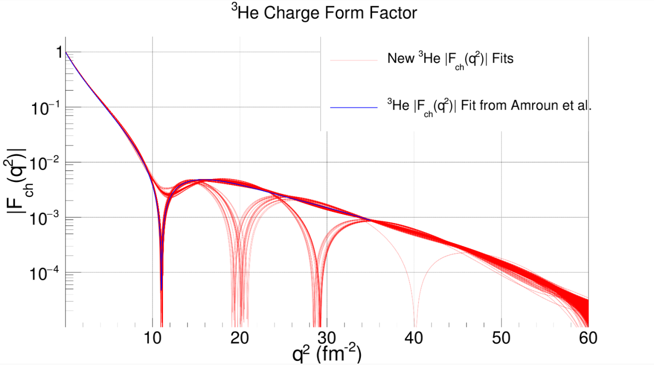

Figure 25: Charge Form Factors from 1352 ^{3}He Fits with no χ^2_{max} cut.

^{3}He Fits

- Let's look at the $N_{Gaus} = 12$ ^{3}He form factor plots.

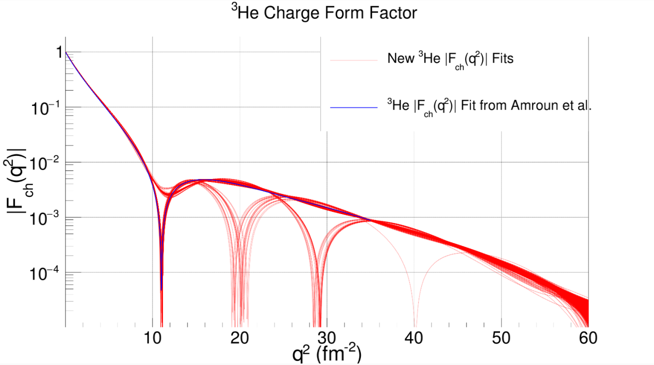

Figure 25: Charge Form Factors from 1352 ^{3}He Fits with no χ^2_{max} cut.

- Many of these fits look nonphysical. How do we remove them?
  - Apply a cut on χ^2.

^{3}He Charge Form Factor

N_{Gaus}	Avg. χ^2	rχ^2	BIC	AIC	$\sum Q_{i_{ch}}$	$\sum Q_{i_m}$	χ^2_{max}	Below Cut
12	523.743	2.23822	249.063	184.771	1.01018	1.04558	No Cut	1352
12	436.564	1.86566	201.908	159.223	1.00840	1.02235	500	852

Table 4: Metrics for Final ^{3}He Fits

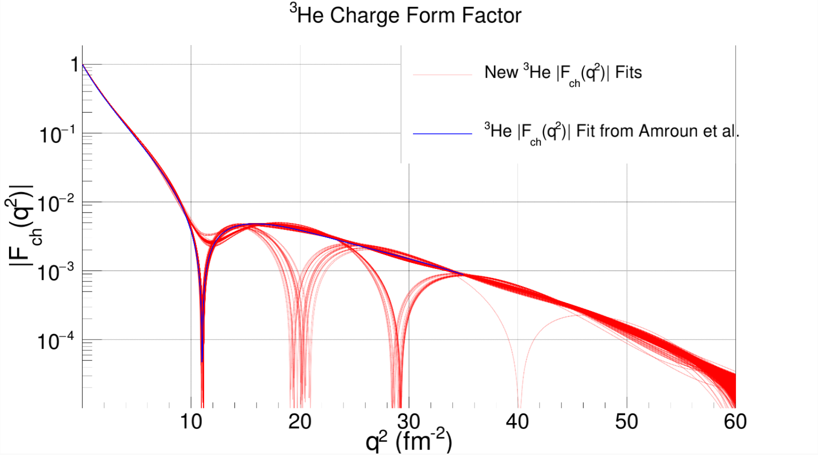

^{3}He Charge Form Factor

N_{Gaus}	Avg. χ^2	rχ^2	BIC	AIC	$\sum Q_{i_{ch}}$	$\sum Q_{i_m}$	χ^2_{max}	Below Cut
12	523.743	2.23822	249.063	184.771	1.01018	1.04558	No Cut	1352
12	436.564	1.86566	201.908	159.223	1.00840	1.02235	500	852

Table 4: Metrics for Final ^{3}He Fits

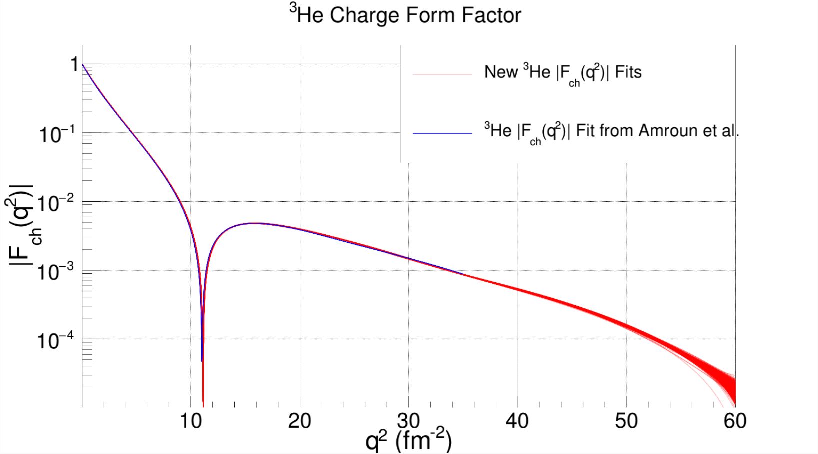

^{3}He Charge Density

- Now we can Fourier transform F_{ch} to find the charge density.

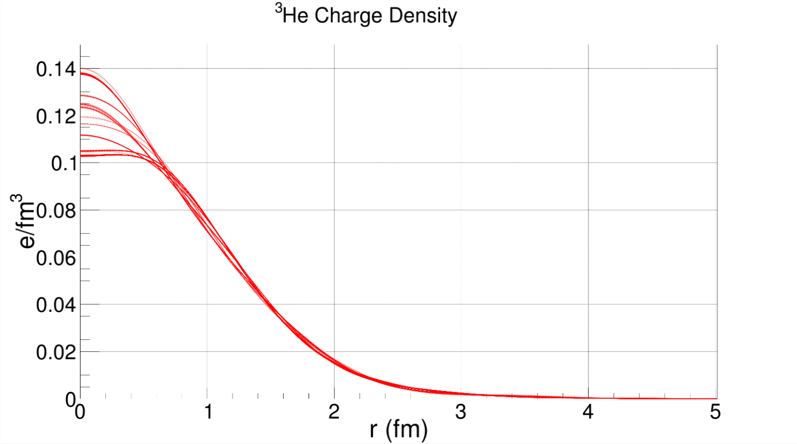

Figure 28: Charge Densities from 1352 ^{3}He Fits with no χ^2_{max} cut.

^{3}He Charge Density

- Now we can Fourier transform F_{ch} to find the charge density.
  - As expected the density falls off by $r = 5$ fm.
  - Density turns over slightly and plateaus at small r.

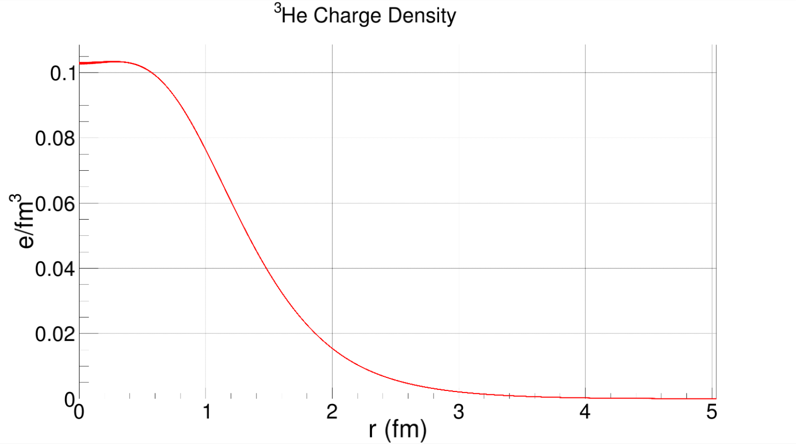

Figure 29: Charge Densities from 852 ^{3}He Fits surviving a $\chi^2_{max} = 500$ cut.

^{3}He Charge Radius

- Using the derivative of F_{ch} we can obtain the charge radius.

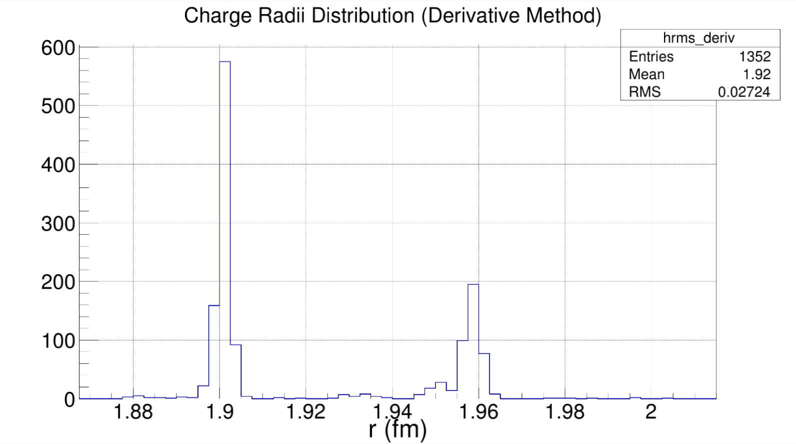

^{3}He Charge Radius

- Using the derivative of F_{ch} we can obtain the charge radius.
  - Higher radii disappear completely with the cut.
  - Avg. ^{3}He charge radius = 1.90 fm, SD = 0.00144 fm.

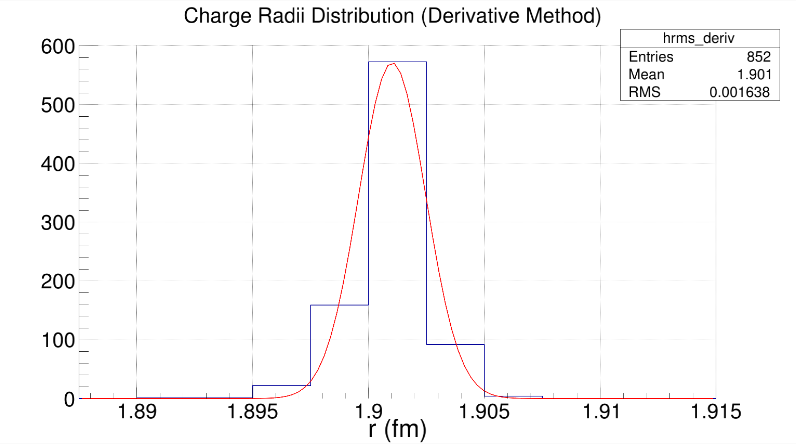

^{3}He Charge Radius

- Using the derivative of F_{ch} we can obtain the charge radius.
  - Higher radii disappear completely with the cut.
  - Avg. ^{3}He charge radius = 1.90 fm, SD = 0.00144 fm.
  - Saclay 1.96 ± 0.03. Bates 1.87 ± 0.03 [10].
  - GFMC 1.97 ± 0.01. χEFT 1.962 ± 0.004 [10].

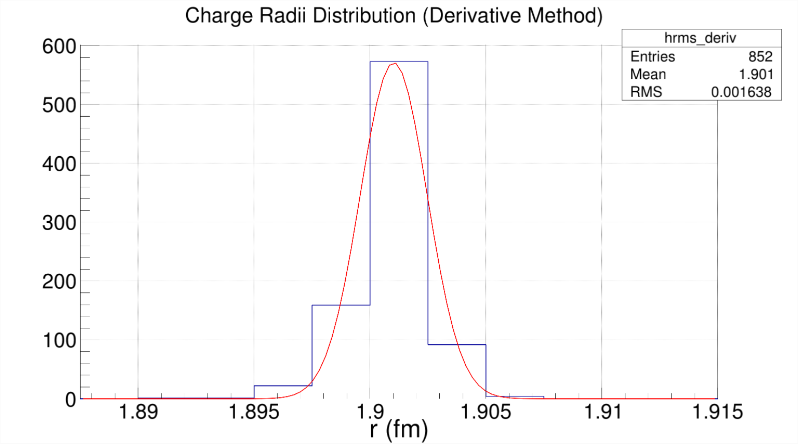

New ^{3}He F_{ch} Fits in Context

- We can compare the new ^{3}He F_{ch} fits to older fits as well as theory [11].

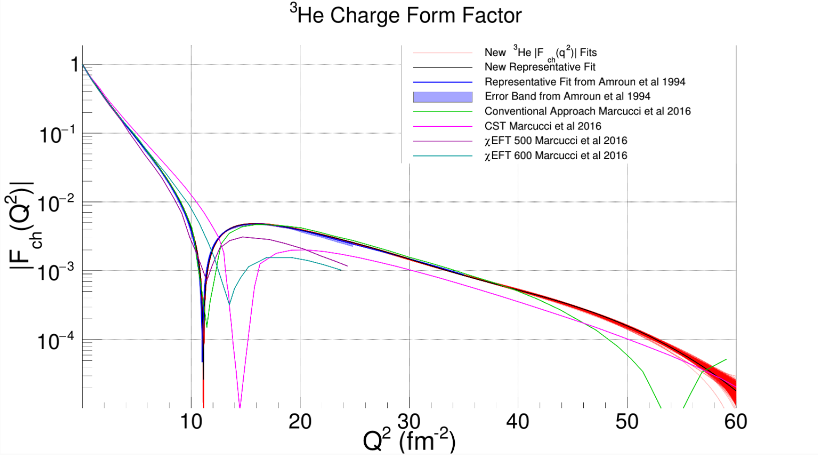

Figure 32: ^{3}He Charge Form Factors.

New ^{3}He F_{ch} Fits in Context Cont.

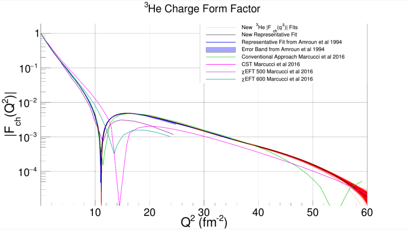

- The F_{ch} fits are very tightly grouped due to an abundance of low Q^2 data.
  - All R_i models strongly agree up to 55-60 fm^{-2}.
- The new fits almost perfectly overlap the fits of Amroun *et al*.

New ^{3}He F_{ch} Fits in Context Cont.

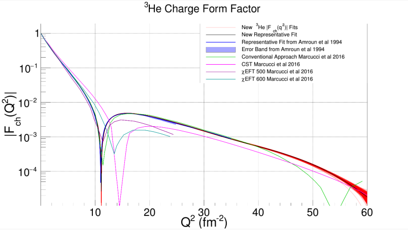

- The F_{ch} fits are very tightly grouped due to an abundance of low Q^2 data.
  - All R_i models strongly agree up to 55-60 fm^{-2}.
- The new fits almost perfectly overlap the fits of Amroun *et al*.

- Conventional Approach: Simulates 2 and 3-body nucleon interactions and relativistic corrections [11].
  - Describes the F_{ch} minima and magnitude very well.

New ^{3}He F_{ch} Fits in Context Cont.

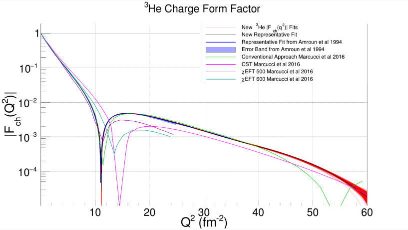

- The F_{ch} fits are very tightly grouped due to an abundance of low Q^2 data.
  - All R_i models strongly agree up to 55-60 fm^{-2}.
- The new fits almost perfectly overlap the fits of Amroun *et al*.

- Conventional Approach: Simulates 2 and 3-body nucleon interactions and relativistic corrections [11].
  - Describes the F_{ch} minima and magnitude very well.
- χEFT: Uses chiral symmetry of QDC to describe the internal strong and EM interactions (momentum space cutoffs 500/600 MeV) [11].
  - Underestimates magnitude of F_{ch}. χEFT500 finds first minima.

New ^{3}He F_{ch} Fits in Context Cont.

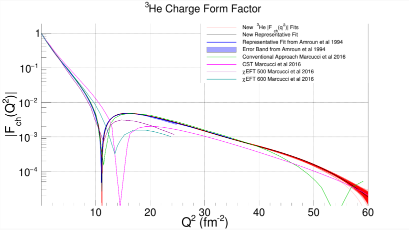

- The F_{ch} fits are very tightly grouped due to an abundance of low Q^2 data.
  - All R_i models strongly agree up to 55-60 fm^{-2}.
- The new fits almost perfectly overlap the fits of Amroun *et al*.

- Conventional Approach: Simulates 2 and 3-body nucleon interactions and relativistic corrections [11].
  - Describes the F_{ch} minima and magnitude very well.
- χEFT: Uses chiral symmetry of QDC to describe the internal strong and EM interactions (momentum space cutoffs 500/600 MeV) [11].
  - Underestimates magnitude of F_{ch}. χEFT500 finds first minima.
- Covariant spectator theorem (CST): Covariant FT where nucleons and light mesons are effective DOF (fully relativistic) [11].
  - Misses F_{ch} minima and underestimates magnitude.

^{3}He Magnetic Form Factor

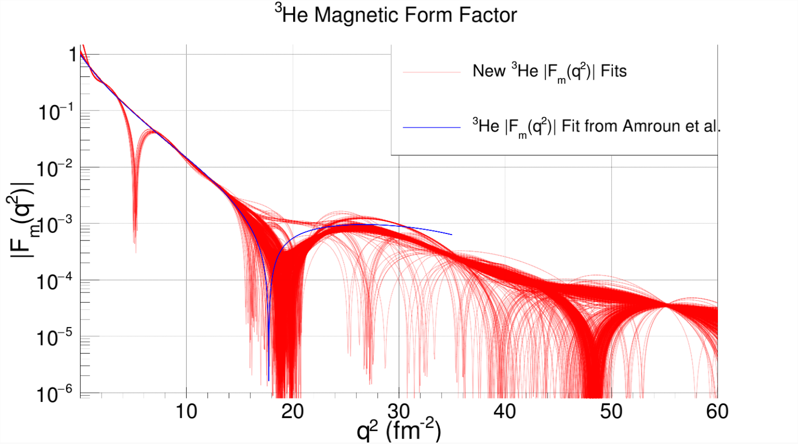

Figure 33: Magnetic Form Factors from 1352 ^{3}He Fits with no χ^2_{max} cut.

^{3}He Magnetic Form Factor

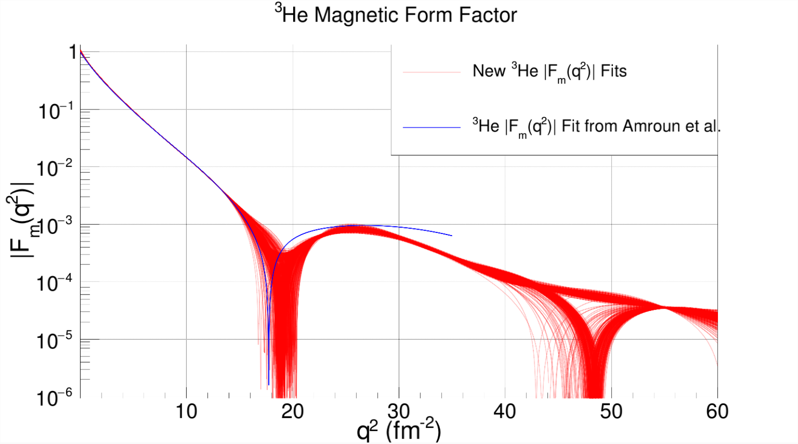

Figure 34: Magnetic Form Factors from 852 ^{3}He Fits surviving a $\chi^2_{max} = 500$ cut.

New ^{3}He F_m Fits in Context

- We can compare the new ^{3}He F_m fits to older fits as well as theory.

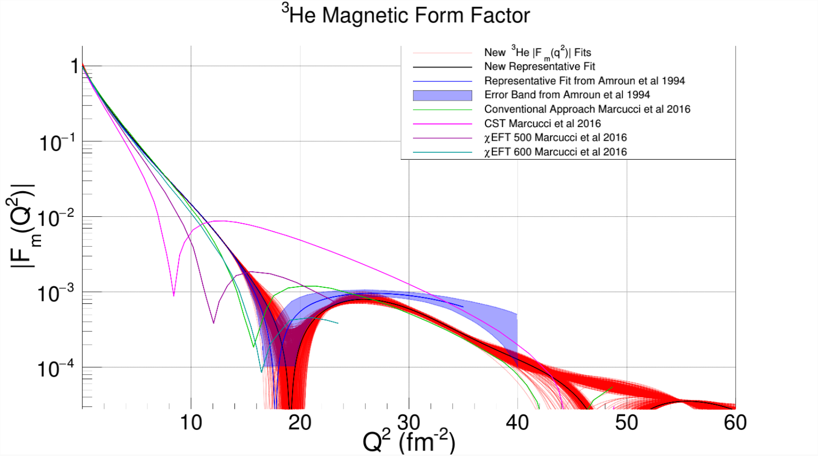

Figure 35: ^{3}**He Magnetic Form Factors.**

New ^{3}He F_m Fits in Context Cont.

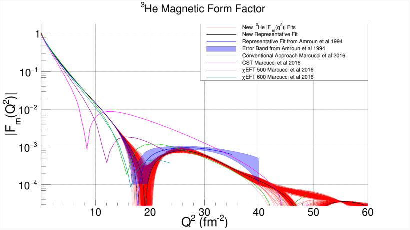

- F_m fits more loosely grouped. Lacking high Q^2 data.
  - The R_i models take divergent paths above 40 fm^{-2}.
- The first minima is shifted back from Amroun *et al*.
- Magnitude decreased between minima.

New ^{3}He F_m Fits in Context Cont.

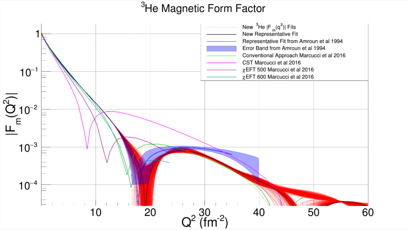

- F_m fits more loosely grouped. Lacking high Q^2 data.
  - The R_i models take divergent paths above 40 fm^{-2}.
- The first minima is shifted back from Amroun *et al*.
- Magnitude decreased between minima.

- Conventional Approach [11]:
  - Minima shifted too low. Appropriate F_m magnitude above 25 fm^{-2}.

New ^{3}He F_m Fits in Context Cont.

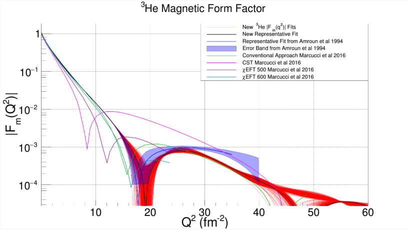

- F_m fits more loosely grouped. Lacking high Q^2 data.
  - The R_i models take divergent paths above 40 fm^{-2}.
- The first minima is shifted back from Amroun *et al*.
- Magnitude decreased between minima.

- Conventional Approach [11]:
  - Minima shifted too low. Appropriate F_m magnitude above 25 fm^{-2}.
- χEFT [11]:
  - χEFT500 misses minima. χEFT600 closest to minima, but underestimates F_m magnitude.

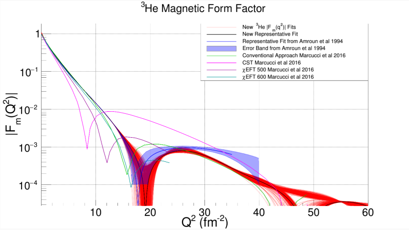

- F_m fits more loosely grouped. Lacking high Q^2 data.
  - The R_i models take divergent paths above 40 fm^{-2}.
- The first minima is shifted back from Amroun *et al*.
- Magnitude decreased between minima.
- Conventional Approach [11]:
  - Minima shifted too low. Appropriate F_m magnitude above 25 fm^{-2}.
- χEFT [11]:
  - χEFT500 misses minima. χEFT600 closest to minima, but underestimates F_m magnitude.
- CST [11]:
  - Very poor description of the data.

New ^{3}He F_m Fits in Context Cont.

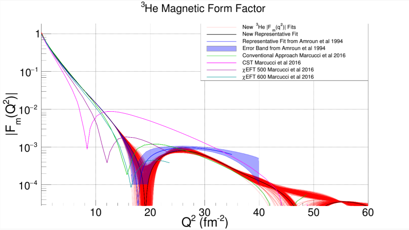

- F_m fits more loosely grouped. Lacking high Q^2 data.
  - The R_i models take divergent paths above 40 fm^{-2}.
- The first minima is shifted back from Amroun *et al*.
- Magnitude decreased between minima.

- Conventional Approach [11]:
  - Minima shifted too low. Appropriate F_m magnitude above 25 fm^{-2}.
- χEFT [11]:
  - χEFT500 misses minima. χEFT600 closest to minima, but underestimates F_m magnitude.
- CST [11]:
  - Very poor description of the data.
- Data first minima moved further away from all predictions.
  - Theory is having difficulty predicting the ^{3}He F_m.

^{3}He Representative Cross Section Fit Statistics

- 259 ^{3}He points. $\chi^2 = 436$. $r\chi^2 = 1.86$.

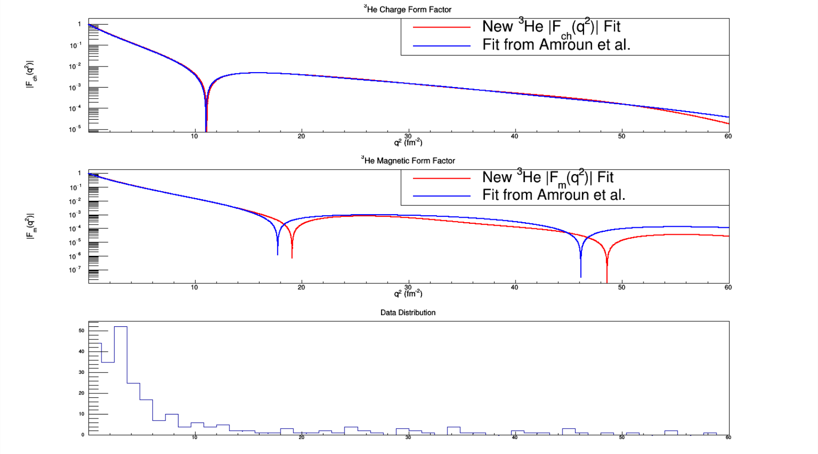

Figure 36: ^{3}**He Representative Form Factors and World Data Distribution.**

^{3}He Representative Cross Section Fit Statistics

- 259 ^{3}He points. $\chi^2 = 436$. $r\chi^2 = 1.86$.

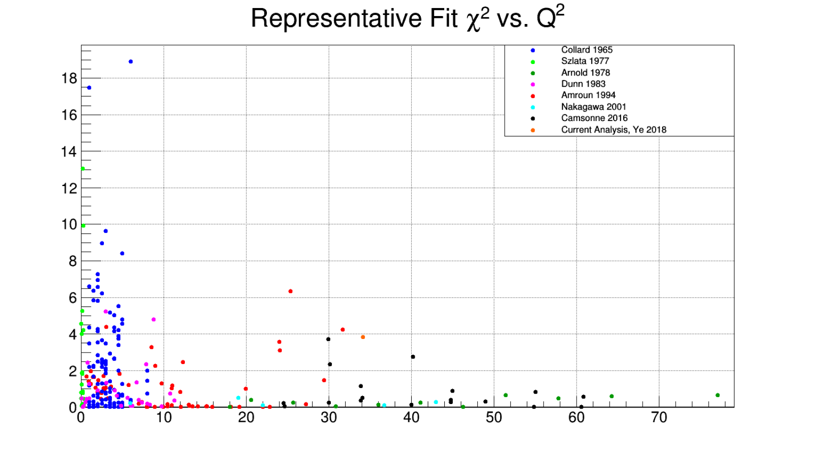

Figure 37: ^{3}**He Representative Fit** χ^2 **vs.** $\mathbf{Q}^2$**.**

^{3}He Representative Cross Section Fit Statistics

- 259 ^{3}He points. $\chi^2 = 436$. $r\chi^2 = 1.86$.

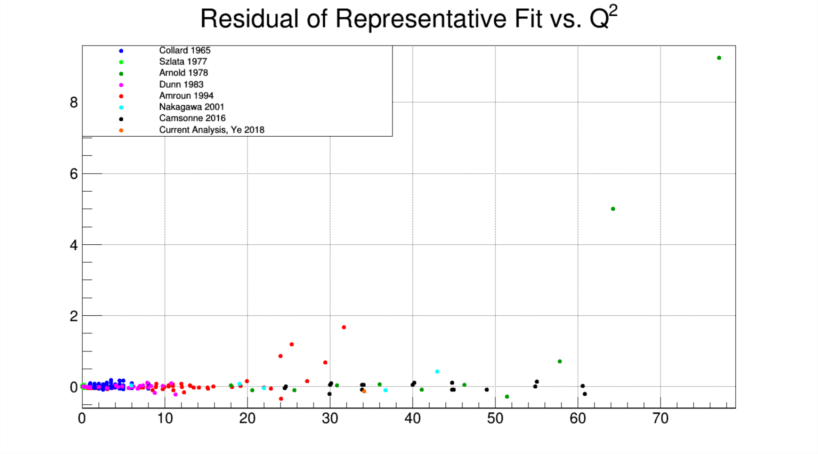

Figure 38: ^{3}He Representative Fit Residual vs. Q^2.

^{3}He Representative Cross Section Fit Statistics

- 259 ^{3}He points. $\chi^2 = 436$. $r\chi^2 = 1.86$.

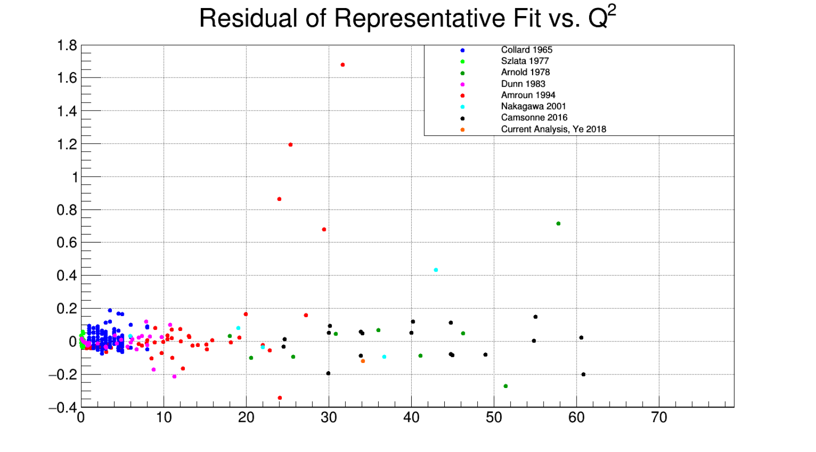

Figure 39: ^{3}He Representative Fit Residual vs. Q^2 Zoomed. Two large residual points from not shown.

^{3}H Charge Form Factor

N_{Gaus}	Avg. χ^2	rχ^2	BIC	AIC	$\sum Q_{i_{ch}}$	$\sum Q_{i_m}$	χ^2_{max}	Below Cut
8	611.385	2.81744	266.175	238.532	1.08866	1.33481	No Cut	2600
8	601.840	2.77346	264.695	237.053	1.08991	1.32926	603	908

Table 5: Metrics for Final ^{3}H Fits

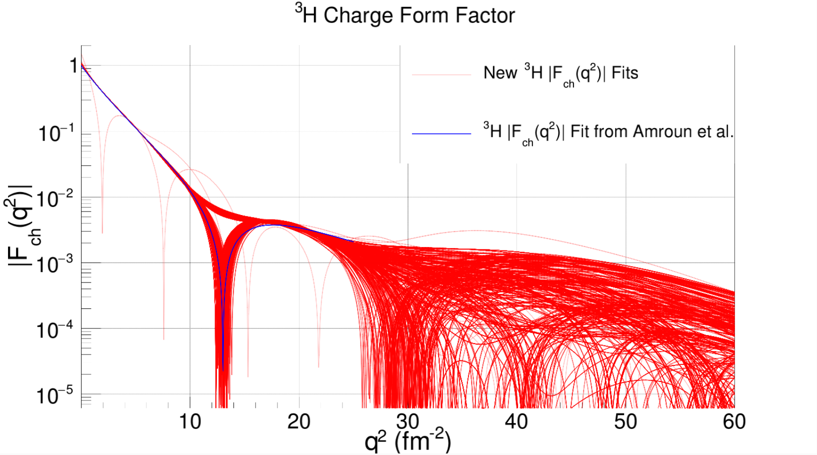

^{3}H Charge Form Factor

N_{Gaus}	Avg. χ^2	$r\chi^2$	BIC	AIC	$\sum Q_{i_{ch}}$	$\sum Q_{i_m}$	χ^2_{max}	Below Cut
8	611.385	2.81744	266.175	238.532	1.08866	1.33481	No Cut	2600
8	601.840	2.77346	264.695	237.053	1.08991	1.32926	603	908

Table 5: Metrics for Final ^{3}H Fits

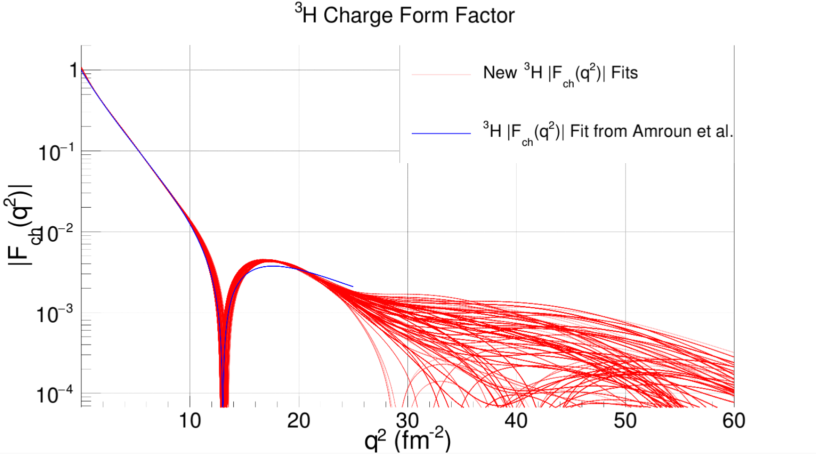

^{3}H Charge Density

- Again we Fourier transform F_{ch} to find the charge density.

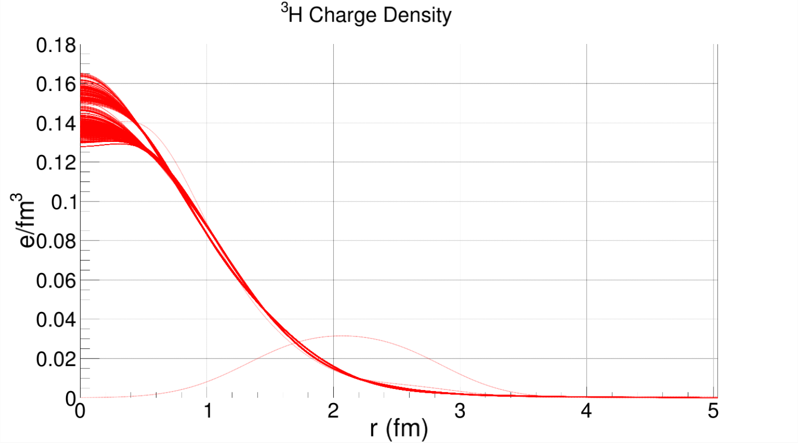

Figure 42: Charge Densities from 2600 ^{3}H Fits with no χ^2_{max} cut.

^{3}H Charge Density

- Again we Fourier transform F_{ch} to find the charge density.
  - Plateaus at small r like ^{3}He. Unclear if the density turns over.
  - Magnitude at $r = 0$ has much more uncertainty than ^{3}He.

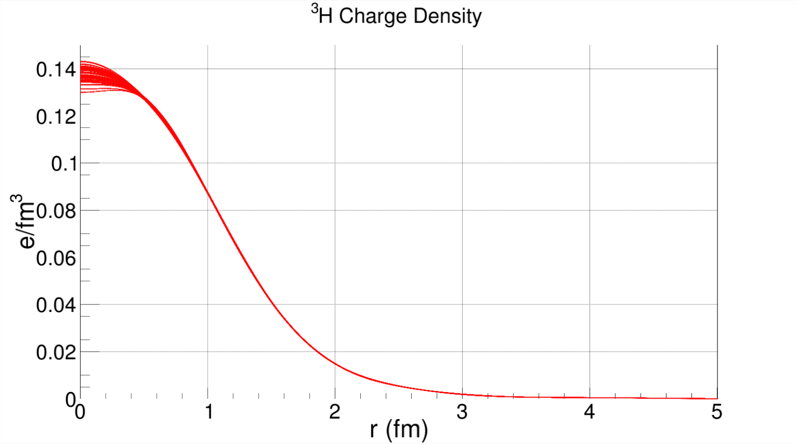

Figure 43: Charge Densities from 908 ^{3}H Fits surviving a $\chi^2_{max} = 603$ cut.

^{3}H Charge Radius

- Again, using the derivative of F_{ch} we can obtain the charge radius.

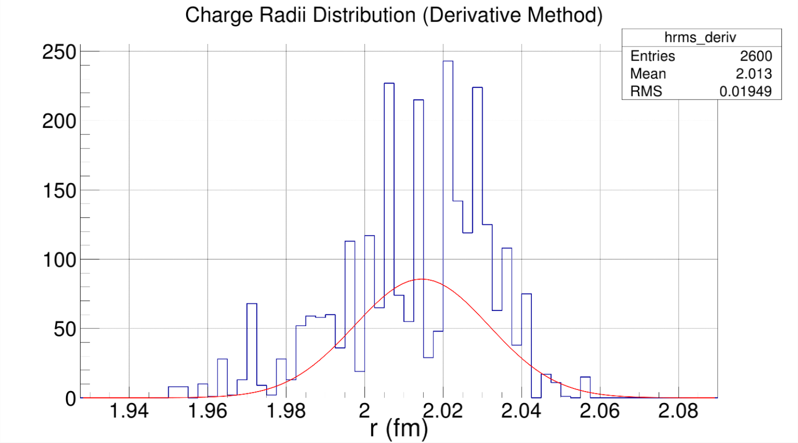

^{3}H Charge Radius

- Again, using the derivative of F_{ch} we can obtain the charge radius.
  - Avg. ^{3}H charge radius = 2.02 fm, SD = 0.0133 fm.

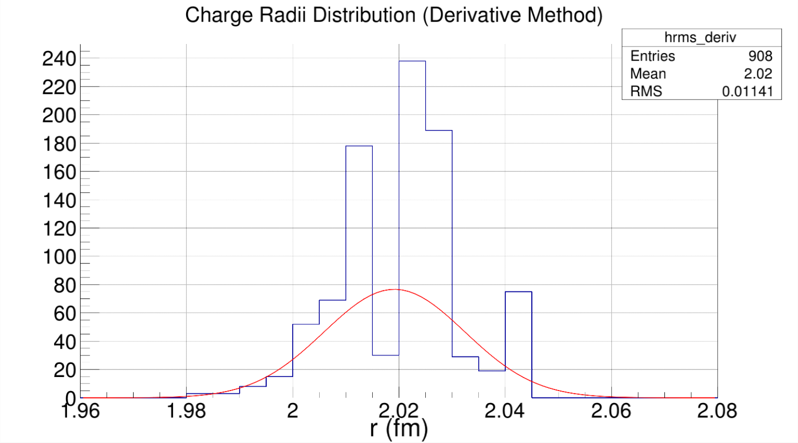

^{3}H Charge Radius

- Again, using the derivative of F_{ch} we can obtain the charge radius.
  - Avg. ^{3}H charge radius = 2.02 fm, SD = 0.0133 fm.
  - Saclay 1.76 ± 0.09. Bates 1.68 ± 0.03 [10].
  - GFMC 1.77 ± 0.01. χEFT 1.756 ± 0.006 [10].

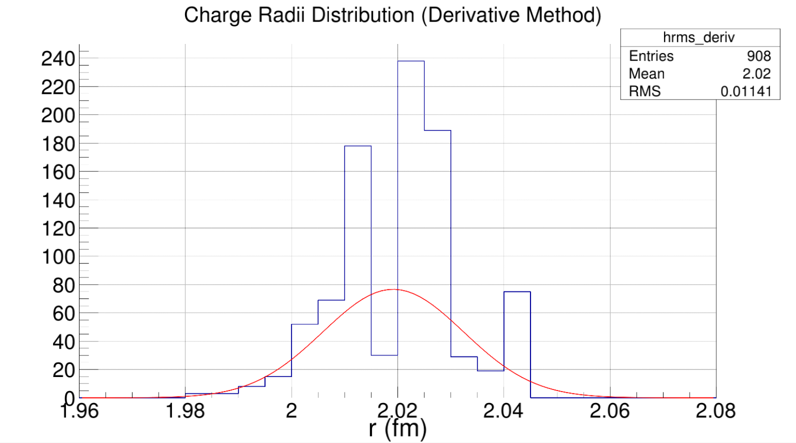

^{3}H Charge Radius

- Again, using the derivative of F_{ch} we can obtain the charge radius.
  - Avg. ^{3}H charge radius = 2.02 fm, SD = 0.0133 fm.
  - Saclay 1.76 ± 0.09. Bates 1.68 ± 0.03 [10].
  - GFMC 1.77 ± 0.01. χEFT 1.756 ± 0.006 [10].
  - This is the result of not forcing $Q_{i_{ch}} = 1$.

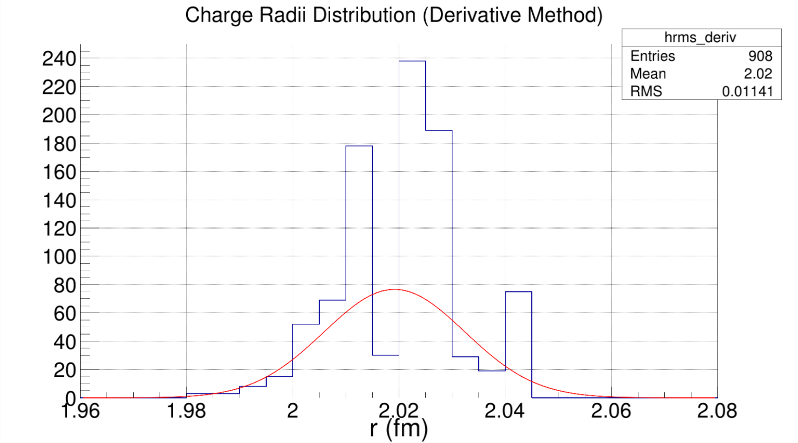

New ^3H F_{ch} Fits in Context

- We can compare the new ^3H F_{ch} fits to older fits.

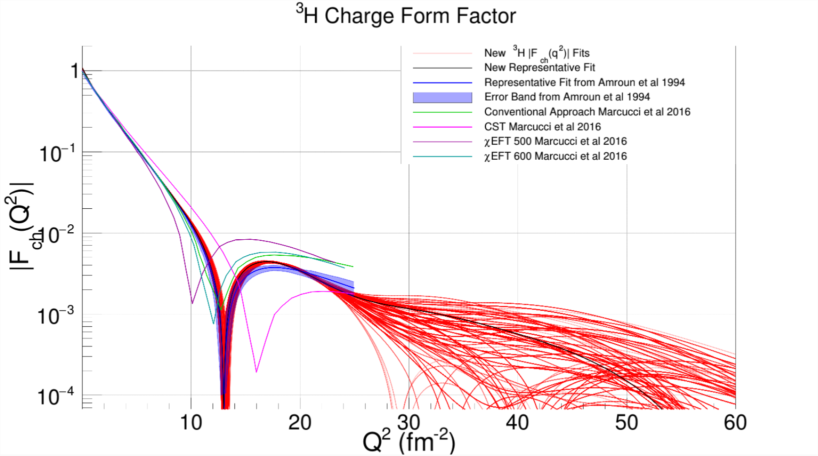

Figure 46: ^3H **Charge Form Factors.**

New ^{3}H F_{ch} Fits in Context Cont.

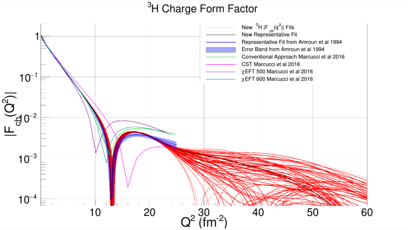

- Results are comparable with Amroun et al.
  - No new ^{3}H data added.
  - Above $Q^2 \approx 25$ fm^{-2} the fits diverge greatly.
- Demonstrates the consistency of our method.

New ^{3}H F_{ch} Fits in Context Cont.

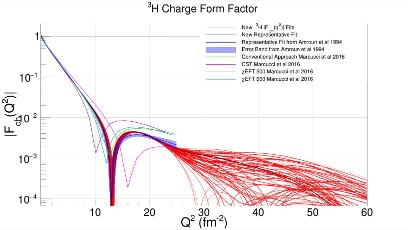

- Results are comparable with Amroun et al.
  - No new ^{3}H data added.
  - Above $Q^2 \approx 25$ fm^{-2} the fits diverge greatly.
- Demonstrates the consistency of our method.
- Conventional Approach [11]:
  - Describes minimum well. F_{ch} magnitude a bit large.

New ^{3}H F_{ch} Fits in Context Cont.

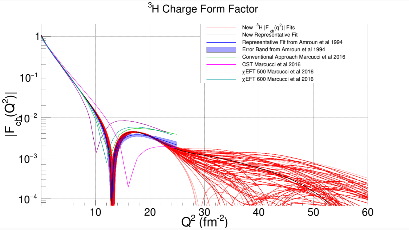

- Results are comparable with Amroun et al.
  - No new ^{3}H data added.
  - Above $Q^2 \approx 25$ fm^{-2} the fits diverge greatly.
- Demonstrates the consistency of our method.

- Conventional Approach [11]:
  - Describes minimum well. F_{ch} magnitude a bit large.
- χEFT [11]:
  - χEFT500 misses minima and magnitude. χEFT600 close to minimum, and slightly large F_{ch} magnitude.

New ^{3}H F_{ch} Fits in Context Cont.

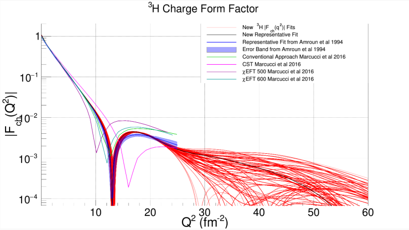

- Results are comparable with Amroun et al.
  - No new ^{3}H data added.
  - Above $Q^2 \approx 25$ fm^{-2} the fits diverge greatly.
- Demonstrates the consistency of our method.

- Conventional Approach [11]:
  - Describes minimum well. F_{ch} magnitude a bit large.
- χEFT [11]:
  - χEFT500 misses minima and magnitude. χEFT600 close to minimum, and slightly large F_{ch} magnitude.
- CST [11]:
  - Poorly describes the data.

New ^{3}H F_{ch} Fits in Context Cont.

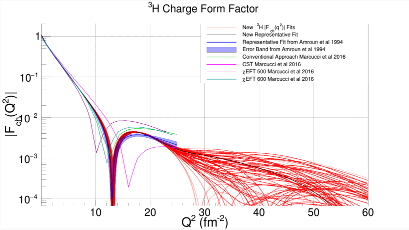

- Results are comparable with Amroun et al.
  - No new ^{3}H data added.
  - Above $Q^2 \approx 25$ fm^{-2} the fits diverge greatly.
- Demonstrates the consistency of our method.

- Conventional Approach [11]:
  - Describes minimum well. F_{ch} magnitude a bit large.
- χEFT [11]:
  - χEFT500 misses minima and magnitude. χEFT600 close to minimum, and slightly large F_{ch} magnitude.
- CST [11]:
  - Poorly describes the data.
- Theory predicts data relatively well.
  - Better understanding of F_{ch} magnitude needed.

^{3}H Magnetic Form Factor

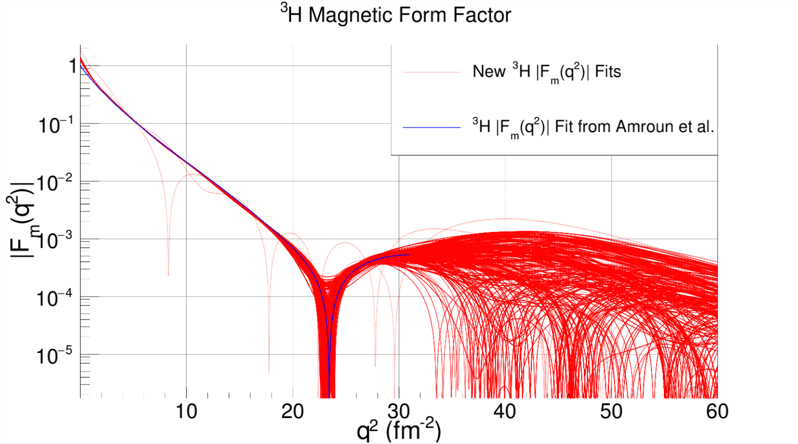

Figure 47: **Magnetic Form Factors from 2600 ^{3}H Fits with no χ^2_{max} cut.**

^{3}H Magnetic Form Factor

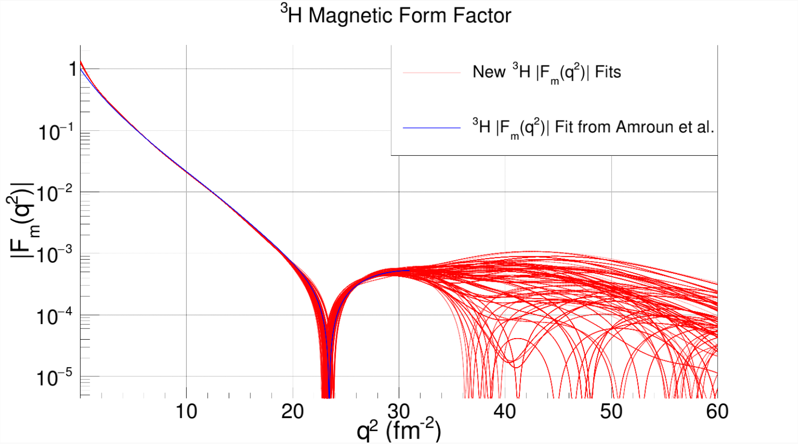

Figure 48: Magnetic Form Factors from 908 ^{3}H Fits surviving a $\chi^2_{max} = 603$ cut.

New ^{3}H F_m Fits in Context

- We can compare the new ^{3}H F_m fits to older fits.

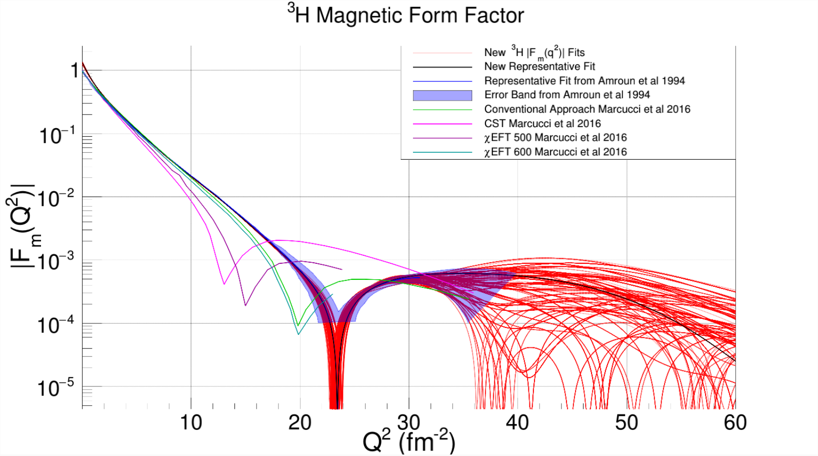

Figure 49: ^{3}H Magnetic Form Factors.

New ^3H F_m Fits in Context Cont.

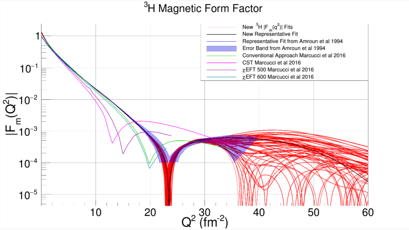

- Results are comparable with Amroun et al.
  - No new ^3H data added.
  - Very little understanding of F_m above $Q^2 = 35$ fm^{-2}.
- Need more high Q^2 data.

New ^3H F_m Fits in Context Cont.

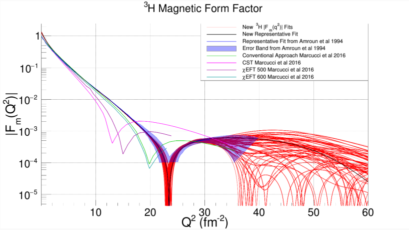

- Results are comparable with Amroun et al.
  - No new ^3H data added.
  - Very little understanding of F_m above $Q^2 = 35$ fm^{-2}.
- Need more high Q^2 data.

- Conventional Approach [11]:
  - Early first minimum. If minimum shifts right F_m magnitude looks close.

New ^3H F_m Fits in Context Cont.

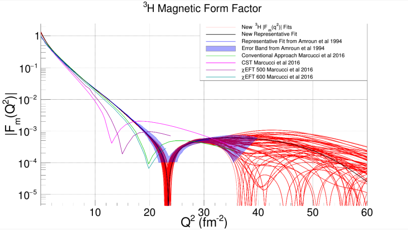

- Results are comparable with Amroun et al.
  - No new ^3H data added.
  - Very little understanding of F_m above $Q^2 = 35$ fm^{-2}.
- Need more high Q^2 data.

- Conventional Approach [11]:
  - Early first minimum. If minimum shifts right F_m magnitude looks close.
- χEFT [11]:
  - χEFT500 misses badly. χEFT600 is similar to the conventional approach.

New ^{3}H F_m Fits in Context Cont.

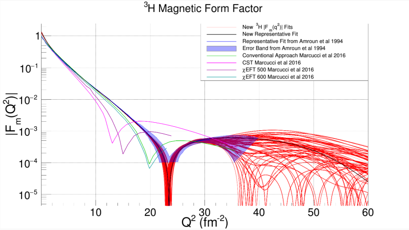

- Results are comparable with Amroun et al.
  - No new ^{3}H data added.
  - Very little understanding of F_m above $Q^2 = 35\ fm^{-2}$.
- Need more high Q^2 data.

- Conventional Approach [11]:
  - Early first minimum. If minimum shifts right F_m magnitude looks close.
- χEFT [11]:
  - χEFT500 misses badly. χEFT600 is similar to the conventional approach.
- CST [11]:
  - Poorly describes the data.

New ^{3}H F_m Fits in Context Cont.

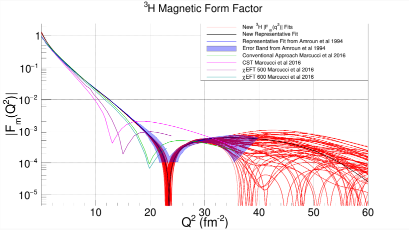

- Results are comparable with Amroun et al.
  - No new ^{3}H data added.
  - Very little understanding of F_m above $Q^2 = 35$ fm^{-2}.
- Need more high Q^2 data.

- Conventional Approach [11]:
  - Early first minimum. If minimum shifts right F_m magnitude looks close.
- χEFT [11]:
  - χEFT500 misses badly. χEFT600 is similar to the conventional approach.
- CST [11]:
  - Poorly describes the data.
- Theory struggles to predict data.
  - Magnitude may be close to correct if minimum shifts up in Q^2.

^{3}H Representative Cross Section Fit Statistics

- 234 ^{3}H points. $\chi^2 = 602$. $r\chi^2 = 2.77$.

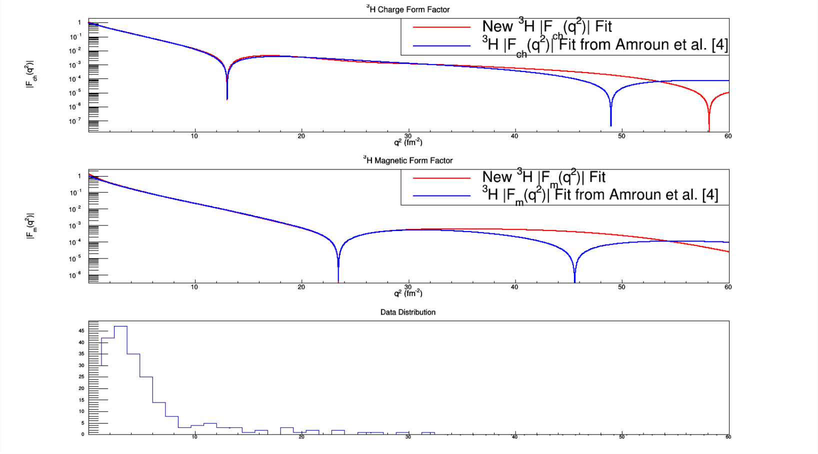

Figure 50: ^{3}**H Representative Form Factors and World Data Distribution.**

^{3}H Representative Cross Section Fit Statistics

- 234 ^{3}H points. $\chi^2 = 602$. r$\chi^2 = 2.77$.

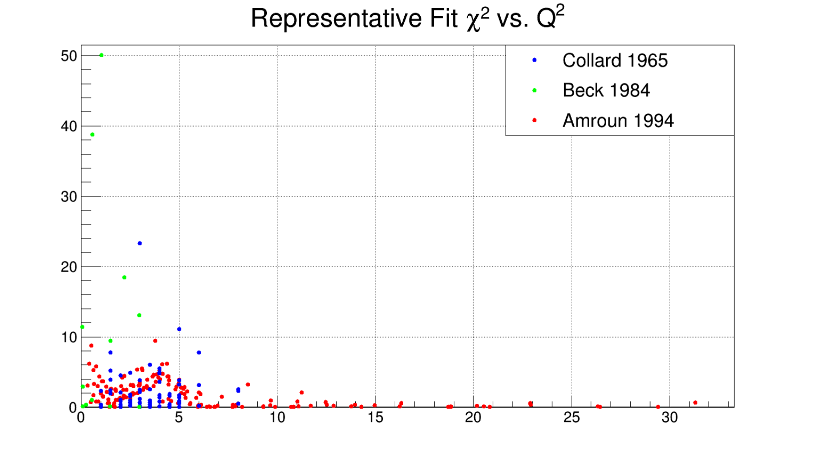

Figure 51: ^{3}H Representative Fit χ^2 vs. Q^2.

^{3}H Representative Cross Section Fit Statistics

- 234 ^{3}H points. $\chi^2 = 602$. $r\chi^2 = 2.77$.

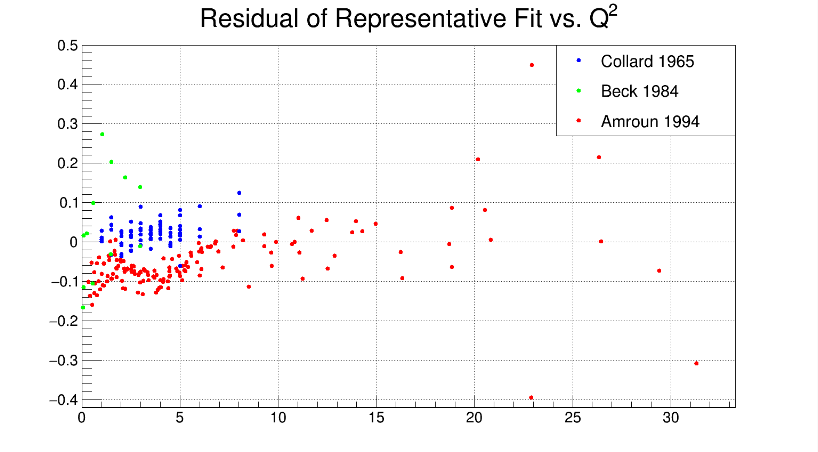

Figure 52: ^{3}H Representative Fit Residual vs. Q^2.

Conclusions

Conclusions

- New ^{3}He elastic cross section of $1.335 \pm 0.086 * 10^{-6}$ μb/sr.

Conclusions

- New ^{3}He elastic cross section of $1.335 \pm 0.086 * 10^{-6}$ μb/sr.
- Modern SOG fits with new JLab and this analysis' data point were performed.
  - ^{3}He F_{ch} and ^{3}H F_{ch} and F_m relatively unchanged.
  - ^{3}He F_m first minimum shift up several fm^{-2} in Q^2.
  - ^{3}He charge radii agrees with past data.
  - ^{3}H charge radii disagrees with past data ($\sum Q_i \neq 1$).

Conclusions

- New ^{3}He elastic cross section of $1.335 \pm 0.086 * 10^{-6}\ \mu b/sr$.
- Modern SOG fits with new JLab and this analysis' data point were performed.
  - ^{3}He F_{ch} and ^{3}H F_{ch} and F_m relatively unchanged.
  - ^{3}He F_m first minimum shift up several fm^{-2} in Q^2.
  - ^{3}He charge radii agrees with past data.
  - ^{3}H charge radii disagrees with past data ($\sum Q_i \neq 1$).
- A conventional theoretical approach using 2 and 3-body nucleon interactions and relativistic corrections reproduces F_{ch} well. χEFT also performs decently.
  - Theory predictions struggle with predicting F_m.

Conclusions

- New ^{3}He elastic cross section of $1.335 \pm 0.086 * 10^{-6}$ μb/sr.
- Modern SOG fits with new JLab and this analysis' data point were performed.
  - ^{3}He F_{ch} and ^{3}H F_{ch} and F_m relatively unchanged.
  - ^{3}He F_m first minimum shift up several fm^{-2} in Q^2.
  - ^{3}He charge radii agrees with past data.
  - ^{3}H charge radii disagrees with past data ($\sum Q_i \neq 1$).
- A conventional theoretical approach using 2 and 3-body nucleon interactions and relativistic corrections reproduces F_{ch} well. χEFT also performs decently.
  - Theory predictions struggle with predicting F_m.
- Need more high Q^2 data to understand form factors beyond the first minimum.
  - JLab is well positioned to make these measurements!
  - Hall A back angle max of 150° with 12 GeV available. Rates fall extremely fast, but very high Q^2 could be accessed.
  - Probe transitional region where scattering off hadrons and mesons $\rightarrow$ scattering off quarks and gluons.

Acknowledgements

- This work was made possible by DOE grant 742481 as well as a JSA Graduate Fellowship.
- Thanks to Douglas Higinbotham for his knowledge of fitting best practices and XS extractions as well as his invaluable mentorship.
- Thanks to Todd Averett for his guidance as my advisor, and the freedom he has allowed me in my research.
- Special thank you to Dien Nguyen for pioneering this data set and saving me countless hours of confusion.
- And thanks to my other JLab mentors like Bob Michaels and Bogdan Wojtsekhowski, and the many others at JLab who have supported me in my graduate work.

Questions

Questions?

References i

1. Povh *et al.*, "Particles and Nuclei an Introduction to the Physical Concepts" (Springer, Reading, Mass, 2008).
2. Z. Ye, "Short Range Correlations in Nuclei at Large x Bj through Inclusive Quasi-Elastic Electron Scattering", (University of Virginia, Dec. 2013).
3. Y. Wang, "Measurement of the Proton Elastic Cross Section at $Q^2 = 0.66, 1.10, 1.51$ and 1.65 GeV^2", (The College of William & Mary, Aug. 2017).
4. D. Nguyen, "Target Density Determination Through Elastic Scattering from ^{3}He in Experiment E08014", unpublished, (Mar. 2016).
5. A. Amroun *et al.*, "^{3}H and ^{3}He EM Form Factors", Nuclear Physics A **579**, 596 (1994).
6. G. Lafferty and T. Wyatt, "Where to stick your data points: The treatment of measurements within wide bins", Nuclear Instruments and Methods in Physics Research Section A **355**, 541 (1995).
7. A. Camsonne *et al.*, "JLab Measurements of the ^{3}He Form Factors at Large Momentum Transfers", Physical Review Letters **119**, (2017).
8. I. Sick, "Model-Independent Nuclear Charge Densities from Elastic Electron Scattering", Nuclear Physics A **218**, 509 (1973).
9. D. Higinbothan, "Bias-Variance Trade-off and Model Selection for Proton Radius Extractions", https://arxiv.org/abs/1812.05706.
10. L. Myers, "E12-14-009: Ratio of the Electric Form Factor in the Mirror Nuclei ^{3}He and ^{3}H", https://arxiv.org/pdf/1408.5283.pdf.
11. L. Marcucci *et al.*, "Electromagnetic Structure of Few-Nucleon Ground States", J. Phys. G: Nucl. Part. Phys. **43**, (2016).